REVIEW ARTICLE: TRANSPORT PHENOMENA AND FLUID MECHANICS

A Review of the Operating Limits in Slot Die Coating Processes

Xiaoyu Ding and Jianhua Liu
School of Mechanical Engineering, Beijing Institute of Technology, Beijing 100081, China

Tequila A. L. Harris
G. W. Woodruff School of Mechanical Engineering, Georgia Institute of Technology, Atlanta, GA 30332

DOI 10.1002/aic.15268
Published online May 4, 2016 in Wiley Online Library (wileyonlinelibrary.com)

Slot die coating is a pre-metered process commonly used for producing thin and uniform films. It is an important film fabrication method for applications where precise coating is required. A major concern in slot die coating processes is how to determine the operating limits to set the appropriate range of operating parameters, including coating speed, flow rate, vacuum pressure, coating gap, liquid viscosity and surface tension, etc. Operating limits directly determine the effectiveness and efficiency of the process. In this article, the current state of academic research on operating limits in slot die coating processes is reviewed. Specifically, the theories, mechanisms, and empirical conclusions related to the limits on vacuum pressure, the low-flow limit, the limit of wet thickness for zero-vacuum-pressure cases, the limit of dynamic wetting failure, and the limits of coating speed for a specific flow rate are reviewed. The article concludes with some recommendations for future work. © 2016 American Institute of Chemical Engineers *AIChE J*, 62: 2508–2524, 2016

Keywords: slot die coating, operating limits, coating window, low flow limit, dynamic wetting failure

Introduction

Slot die coating is a versatile process that is widely used for producing thin and uniform films. It was invented by Beguin[1] for the production of photographic films and papers. During the conventional slot die coating process, a liquid is delivered through a fixed slot gap onto a moving substrate, filling the gap between the die and the substrate or the coating gap. The liquid in the coating gap bounded by the upstream and downstream menisci forms the coating bead. A liquid layer over the moving substrate is carried away from the downstream meniscus. After evaporation or solidification, a uniform dry film can be obtained on the substrate. A major benefit of slot die coating is that it is a pre-metered process, which means that the thickness of the coated liquid layer or wet thickness can be preset and precisely controlled based on the flow rate of the liquid fed into the die and the substrate speed or coating speed. The wet thickness is independent of other process variables.[2] Thus, slot die coating is an important film fabrication method for applications where precise coating is required.

The wet thickness of the coated liquid layer in the traditional slot die coating process can vary from 10 to a few hundred microns and the coating speed can be as high as 2 m/s,[3] while with a tensioned-web-over-slot die (TWOSD) coating process, a wet thickness of less than 5 μm can readily be obtained.[4,5] Traditionally, slot die coating has been used for fabricating photographic films, magnetic tapes, optical films, and many other products. The effectiveness of slot die coating has also been demonstrated in the manufacturing of thin films and electrodes in polymer electrolyte membrane fuel cells,[6,7] solar cells,[8,9] and lithium-ion batteries.[10,11] Recently, slot die coating has attracted increased attention for fabricating thin organic films for flexible organic electronics.[12,13]

A major concern in slot die coating processes is how to determine the operating limits to set the appropriate range of operating parameters, including coating speed, flow rate, vacuum pressure, coating gap, liquid viscosity and surface tension, etc. Outside the proper ranges, coating defects will occur, such as ribbing, dripping, rivulets, and air entrainment. More details about coating defects can be found in several textbooks.[14,15] Determining the operating limits for slot die coating processes are a very complex issue. Several relevant concepts can be found in existing studies, such as low-flow limit, minimum wet thickness, coating window, and maximum wetting speed. These concepts describe the operating limits of the slot die coating process in different respects. Despite much research work over several decades, the mechanisms underlying the operating limits in the slot die coating process remain only partially understood. This restricts our ability to optimize operating parameters for the process.

This incomplete understanding stems from many factors. First, the operating limits are determined by a complex set of competing forces that act on the coating bead, including capillary, viscous, applied vacuum pressure, inertial, gravitational, and elastic forces.[16,17] These forces are significantly affected by geometric variables and material properties, making it difficult to evaluate them precisely. Second, materials used in the

Correspondence concerning this article should be addressed to X. Ding at xiaoyu.ding@bit.edu.cn.

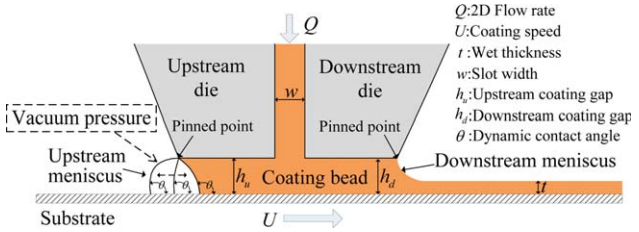

Figure 1. Capillary coating bead with upstream meniscus pinned.

[Color figure can be viewed in the online issue, which is available at wileyonlinelibrary.com.]

coating industry are diverse and their characteristics and properties span a wide range. Specifically, the coating fluids in industry can be Newtonian, but are usually polymer solutions or colloidal suspensions.[16] Their rheological properties may be shear-shinning, extension-thickening, or viscoelastic.[16] Generally, the viscosity of coating fluids can vary from 1 mPa-s to several kPa-s, and the surface tension can range from less than 25 mN/m to more than 500 mN/m.[18] The substrate material can also vary among different polymers, composites, or metals.[18] The diversity of materials has resulted in diverse experimental phenomena, which cannot be uniformly explained by one theory.

In the following sections, the current state of academic research on the operating limits in the slot die coating process is reviewed. This survey is not intended to be exhaustive; the aim is to develop a comprehensive vision for the operating limits of slot die coating processes, and this reflects our perspective on current progress. This review focuses mainly on the single-layer slot die coating process. This type of slot die coating is the most commonly studied and the theories, mechanisms, and empirical conclusions are generally applicable to many industrial scenarios. Studies on operating limits of double-layers slot die coating (with a fixed coating gap or over a tensioned web[19,20]) are relatively rare in the literature,[21] thus is not discussed explicitly in the current study. The article concludes with some recommendations for future work.

Capillary Model of Operating Limits

Operating limits in slot die coating are used to set the appropriate ranges of operating parameters. If operating parameters are within the proper ranges, the coating bead will be stable and the coated layer can be expected to be defect-free, whereas outside the proper ranges, the coating bead will be unstable and coating defects will likely occur. To improve the stability of the coating bead, reduced pressure or vacuum is usually applied to the upstream meniscus, as shown in Figure 1. This method was first suggested by Beguin[1] who invented a vacuum box to apply the vacuum. Later, others introduced a vacuum slot to replace the vacuum box.[3,22]

The first theoretical study of operating limits in slot die coating was provided by Ruschak[23] who analyzed the stability of the coating bead when a vacuum was applied. Based on an extension of the Landau–Levich[24] film coating theory, Ruschak provided analytical ranges for the vacuum pressure and the wet thickness for a stable coating bead. Ruschak's analysis was based on the assumption that the viscous effects are relatively small, and the operating limits are set mainly by capillary pressure in the coating bead. Thus, Ruschak's model of operating limits can be thought of as a capillary model. In this capillary model, the operating limits are given by

$$-\frac{\sigma_u(1+\cos\theta)}{h_u}+1.34Ca^{\frac{2}{3}}\frac{\sigma_d}{t}\le\Delta p\le\frac{\sigma_u(1-\cos\theta)}{h_u}+1.34Ca^{\frac{2}{3}}\frac{\sigma_d}{t} \quad (1)$$

$$0\le\frac{1}{t}\le\frac{1.49}{h_d}Ca^{-\frac{2}{3}} \quad (2)$$

where inequalities (1) and (2) set the limits of vacuum pressure and wet thickness, respectively. Here, σ_u and σ_d are the surface tensions at the upstream and downstream menisci, respectively. Δp represents the vacuum pressure between the upstream and downstream menisci (i.e., the pressure outside the downstream meniscus minus the pressure outside the upstream meniscus). Ca is the capillary number, $\frac{\mu U}{\sigma_d}$, based on the downstream surface tension. μ is the viscosity of the coating fluid. Because the downstream meniscus is always under atmospheric conditions in practice, σ_d actually represents the surface tension in the atmosphere. Other nomenclature in inequalities (1) and (2) are the same as those shown in Figure 1. It should be noted that inequalities (1) and (2) as presented here, in fact, follow Higgins and Scriven's[25] derivation, which has some slight modifications compared with Ruschak's original work.[23] Specifically, in Ruschak's derivation, the coating gap and surface tension did not vary between the upstream and downstream menisci: i.e., $h_u=h_d$ and $\sigma_u=\sigma_d$.

The derivation of inequality (1) can be explained in the following way. The upstream meniscus is assumed to be an arc of a circle and pinned at the upstream corner of the die, as shown in Figure 1. The dynamic contact angle is assumed to be a constant value. In this case, based on simple geometric arguments, the upstream arc can be concave or convex (as indicated in Figure 1). Additionally, the radius of the upstream arc can vary only in a specific range,[25] from which the range of capillary pressure at the upstream meniscus can be established. Then, inequality (1) can be obtained by the balance of pressure across the coating bead.

From a practical viewpoint, vacuum pressure is generally not a real restriction in industrial production, because it can be adjusted to any desired value. In addition, the dynamic contact angle, θ, in inequality (1) is unknown, so inequality (1) is practically less useful than inequality (2), which sets the minimum wet thickness that can be achieved in the slot die coating process. The minimum wet thickness is a crucial operating limit because it largely reflects the effectiveness of the coating process. The derivation of inequality (2) is based on the Landau–Levich boundary condition[23]:

$$\Delta p_t=1.34Ca^{\frac{2}{3}}\frac{\sigma_d}{t} \quad (3)$$

where Δp_t is the capillary pressure. The Landau–Levich boundary condition was derived based on the assumption that both flow rate and coating speed are approaching zero.[23,24] Thus, it is valid only for small capillary and Reynolds numbers. A detailed discussion of the basic ideas underlying the Landau–Levich boundary condition can be found in Ruschak's review.[26]

Like the upstream meniscus, the downstream meniscus is also assumed to be an arc of a circle and pinned at the downstream corner of the die, and can be at a tangent to the moving substrate, as shown in Figure 1. In this case, the radius of the downstream arc can vary between $\frac{h_d}{2}$ and infinity: thus, Δp_t can vary between $\frac{2\sigma_d}{h_d}$ and zero, based on the Young-Laplace

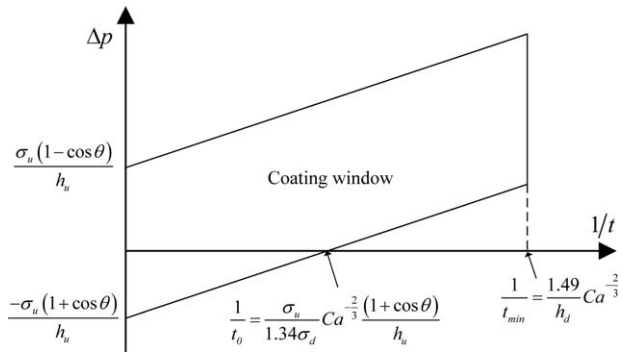

Figure 2. Operating region for a capillary coating bead at a given capillary number (recreated based on Refs. 23, 25).

equation. Combining the range of Δp_t and Eq. 3 results in inequality (2). Based on the analysis above, the minimum wet thickness, t_{min}, that can be achieved in the slot die coating process corresponding to the minimum radius of the downstream arc, can be obtained from inequality (2):

$$t_{min}=0.67h_dCa^{\frac{2}{3}} \tag{4}$$

Equation 4 is an important conclusion from the capillary model of operating limits.[25] It shows that the minimum wet thickness is simply a function of the capillary number and downstream coating gap. In particular, it is independent of the upstream coating gap, which is an important conclusion for the design of die configurations. A direct demonstration of this conclusion can be found in Quinones et al.'s[27] numerical study of operating limits using different die lip configurations.

The capillary model of operating limits given by inequalities (1) and (2) can be plotted, as in Figure 2. They form a region for stable coating, which has been referred to as a coating window,[25] a term found in many existing studies. Generally, it represents the region of stable coating without defects in the space of operating parameters.[2] As will be discussed in the following sections, the coating windows are usually presented as two-dimensional (2D) plots to ease the visualization and understanding. However, an individual 2D plot cannot reflect the range of all operating parameters. Thus, depending on the specific parameters considered, the coating window can be presented as different forms of plot.

In the operating region shown in Figure 2, the upper and lower boundaries are described by inequality (1), which, respectively, reflects the upper and lower limits of vacuum pressure. It can be seen from Figure 2 that the upper limit of vacuum pressure does not cross the coordinate line of $1/t$. This means that the wet thickness could be infinitely large (i.e., $1/t=0$) when the vacuum pressure is zero, which cannot be true in practice. A main reason for this error is that the Landau–Levich film coating theory, used for the derivation of inequality (1), is valid only for thin coating thicknesses.[23] Thus, inequality (1) does not give good approximations for relatively large wet thicknesses.

The right-most boundary in Figure 2 is usually referred as the *low-flow limit*[2,16,28]: the minimum wet thickness for a specified capillary number and downstream coating gap. Because the wet thickness is pre-metered by the ratio of the flow rate to the coating speed, i.e., Q/U, the low-flow limit is also an upper bound of the coating speed for a given flow rate. It has to be clarified that the flow rate in this article and most existing studies is a 2D flow rate in the cross-section shown in Figure 1, measured in m^2/s.

Another important result that can be obtained from the capillary model of operating limits is the expression of the thinnest film thickness when Δp is zero, which is denoted by t_0 (as indicated in Figure 2) and given by

$$t_0=\frac{1.34\sigma_d}{\sigma_u}Ca^{\frac{2}{3}}\frac{h_u}{(1+\cos\theta)} \tag{5}$$

t_0 is also an important limit for practical operations. Equation 5 is directly derived from the left side of inequality (1). An interesting finding from Eqs. 4 and 5 is that both t_{min} and t_0 increase with capillary number to the power of $2/3$. Equations 4 and 5 were derived based on the assumption of pinning the upstream meniscus at the upstream corner of the die (as shown in Figure 1). Higgins and Scriven[25] also realized this assumption and studied a capillary coating bead with a free upstream meniscus. In that case, t_{min} is the same as Eq. 4; t_0 still increases with capillary number to the power of $2/3$, but the specific expression is slightly different.

Viscous Model of Operating Limits

Higgins and Scriven[25] studied the operation limits where capillary effects (surface tension effects) were ignored. In this case, operating limits are set only by viscous pressure in the coating bead. Higgins and Scriven[25] studied this problem by assuming that the upstream meniscus was free to move. As shown in Figure 3, the position of the upstream meniscus can move from the upstream edge of the upstream die lip to the downstream edge of the upstream die lip. When the upstream meniscus moves to the downstream edge of the upstream die lip, the top boundary of the upstream meniscus is pinned at the corner of the upstream die lip and cannot move any further downstream. Increasing the coating speed (or decrease in the vacuum pressure) will cause instability of the coating bead and lead to defects such as cross-web periodic thickness variation and air bubbles. However, when the upstream meniscus moves to the upstream edge of the upstream die lip, a further decrease in the coating speed (or increase in the vacuum pressure) will cause the upstream meniscus to move out of the die lip. This usually leads to the defect called dripping.

More discussion on coating defects related to slot die coating can be found in the section titled *a brief discussion on coating defects related to operating limits*. The viscous flow in the coating bead is approximately a combination of the Couette and the Poiseuille contributions. By applying lubrication theory to the upstream and downstream channels, the pressure difference between upstream and downstream menisci (i.e., the vacuum pressure), Δp, can be expressed as a function of

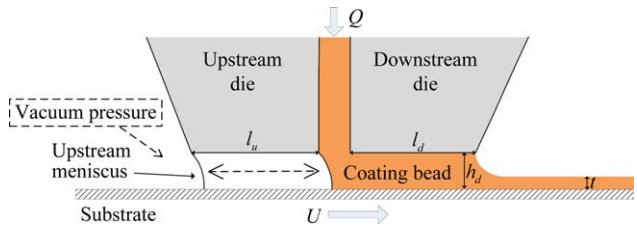

Figure 3. Viscous coating bead with upstream meniscus free.

[Color figure can be viewed in the online issue, which is available at wileyonlinelibrary.com.]

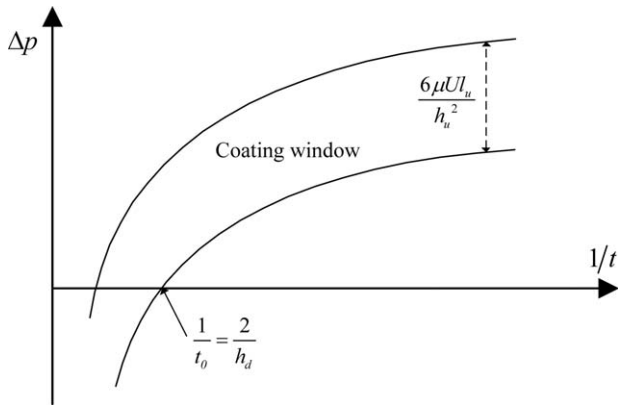

Figure 4. The operating region for a viscous coating bead (recreated based on Ref. 25).

the position of the upstream meniscus.[25] Then, based on the position of the upstream meniscus, a range of Δp can be given as

$$\frac{6\mu U l_d}{{h_d}^2}\left[1-\frac{2t}{h_d}\right] \le \Delta p \le \frac{6\mu U l_d}{{h_d}^2}\left[1+\frac{l_u {h_d}^2}{l_d {h_u}^2}-\frac{2t}{h_d}\right] \tag{6}$$

where l_u and l_d are the lip lengths of the bottom surface of the upstream and downstream dies, as shown in Figure 3. Inequality (6) is the viscous model of limits of vacuum pressure in the slot die coating process. Because capillary effects have been ignored, the Landau–Levich boundary condition is not valid; thus, there is no low-flow limit in this situation. The allowable coating region restricted by inequality (6) is plotted in Figure 4. The lower and upper bounds of this region correspond to the left and right sides of inequality (6), respectively; it can be seen that there is no right bound of this region.

An important result that can be obtained from inequality (6) is that t_0 for a viscous coating bead is simply half of the downstream coating gap:

$$t_0 = \frac{h_d}{2} \tag{7}$$

Equation 7 is arrived at by making the left side of the inequality (6) equal zero. Equation 7 means that for a viscous coating bead, t_0 depends only on the downstream coating gap, and is independent of capillary number. This is apparently different from Eq. 5 for a capillary coating bead.

Viscocapillary Model of Operating Limits

When neither capillary nor viscous pressure can be ignored in the coating bead, the operating limits will be more complex. Higgins and Scriven[25] first studied this case, and referred to the coating bead as a viscocapillary one. For a viscocapillary coating bead, both capillary and viscous pressures in the coating bead govern the operating limits. Hence, the operating region is a state combining the capillary and viscous cases above, as shown schematically in Figure 5.

Because the Landau–Levich boundary condition is still assumed to be valid in this case, the low-flow limit, t_{min}, of the viscocapillary coating bead is the same as Eq. 4. However, the models of Δp and t_0 are more complex. Higgins and Scriven[25] obtained explicit expressions of Δp and t_0 for the viscocapillary case by assuming the upstream meniscus is pinned at the upstream corner of the upstream die lip:

$$\begin{aligned}\Delta p &\ge \frac{6\mu U l_d}{{h_d}^2}\left[1+\frac{l_u {h_d}^2}{l_d {h_u}^2}-\frac{2t}{h_d}\right]+1.34Ca^{\frac{2}{3}}\frac{\sigma_d}{t}-\frac{\sigma_u(1+\cos\theta)}{h_u}\\ \Delta p &\le \frac{6\mu U l_d}{{h_d}^2}\left[1+\frac{l_u {h_d}^2}{l_d {h_u}^2}-\frac{2t}{h_d}\right]+1.34Ca^{\frac{2}{3}}\frac{\sigma_d}{t}+\frac{\sigma_u(1-\cos\theta)}{h_u}\end{aligned} \tag{8}$$

Thus,

$$\begin{aligned}t_0 = \frac{1.34\sigma_d}{\sigma_u}Ca^{\frac{2}{3}}\frac{h_u}{(1+\cos\theta)}\Bigg[1+\frac{6Ca}{1+\cos\theta}\frac{l_d}{h_d}\\ \times\frac{\sigma_d}{\sigma_u}\frac{h_u}{h_d}\left(1+\frac{l_u}{l_d}\frac{{h_d}^2}{{h_u}^2}-\frac{2.68\sigma_d}{\sigma_u}Ca^{\frac{2}{3}}\frac{h_u}{(1+\cos\theta)h_d}\right)\Bigg]\end{aligned} \tag{9}$$

However, the assumption of pinning the upstream meniscus is too rigorous. For a free upstream meniscus, the range of Δp for a viscocapillary coating bead can be given based on the range of position of the upstream meniscus[29,30]:

$$\begin{aligned}\Delta p &\ge \frac{6\mu U l_d}{{h_d}^2}\left[1-\frac{2t}{h_d}\right]+1.34Ca^{\frac{2}{3}}\frac{\sigma_d}{t}-\frac{\sigma_u(\cos\theta+\cos\theta_s)}{h_u}\\ \Delta p &\le \frac{6\mu U l_d}{{h_d}^2}\left[1+\frac{l_u {h_d}^2}{l_d {h_u}^2}-\frac{2t}{h_d}\right]+1.34Ca^{\frac{2}{3}}\frac{\sigma_d}{t}-\frac{\sigma_u(\cos\theta+\cos\theta_s)}{h_u}\end{aligned} \tag{10}$$

where θ_s is the static contact angle between the upstream meniscus and the die lip surface. The expression of t_0 for a free upstream meniscus can also be arrived at by making the lower limit in inequality of (10) equal zero. The specific expression is not explicitly given here.

Based on the discussion above, it can be seen that both the capillary and viscocapillary models of operating limits are functions of capillary number. Thus, the shape and/or position of the operating regions shown in Figures 2 and 5 will change with varying capillary number. Additionally, because the capillary and viscocapillary models of operating limits are based on the Landau–Levich boundary condition, they are valid only for small capillary and Reynolds numbers.[2,23,24] As will be discussed in the following sections, when the capillary number is relatively high, t_{min} and t_0 will show completely different characteristics when compared with the low capillary region.

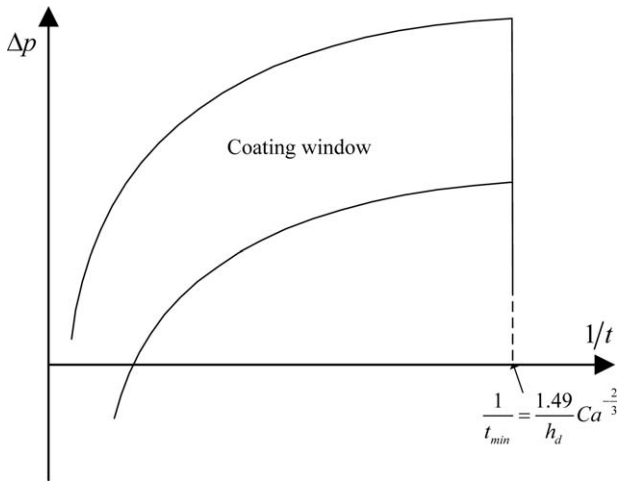

Figure 5. Operating region for a viscocapillary coating bead at a given capillary number (recreated based on Ref. 25).

Much work has been done to study the characteristic regions of t_{min} and t_0.[2,17,31,32] In some studies, t_0 has been referred to as the "minimum wet thickness", which may seem like the definition of t_{min}.[17,31,32] However, based on theoretical derivations, t_{min} and t_0 have apparently different physical meanings. Specifically, t_{min} is related to the movement of the downstream meniscus, whereas t_0 is related to the movement of upstream meniscus. t_{min} occurs when the downstream meniscus is so curved that it cannot bridge the coating gap.[28] t_0 occurs when the upstream meniscus is stretched too much to remain stable. Some photographs showing the position and shape of the menisci at these two limits can be found in the reports of Romero et al.[28] and Bhamidipati et al.[33]

Since t_{min} and t_0 correspond to the minimum wet thickness with and without using vacuum pressure, respectively. The ratio of t_{min}/t_0 can be used to evaluate the effectiveness of vacuum pressure, as used by Lee et al.[31] A smaller ratio of t_{min}/t_0 means higher effectiveness of vacuum pressure. In practice, an important factor affecting the effectiveness of vacuum pressure is viscosity. Since the viscocapillary model for t_0 is very complex, it is difficult to assess the trend of t_{min}/t_0 from it. However, it is possible to assess the general trend of t_{min}/t_0 based on the capillary and viscous models of t_0. Specifically, based on the capillary model of t_0 (Eq. 5), the ratio of t_{min}/t_0 does not change with viscosity; whereas based on the viscous model of t_0 (Eq. 7), the ratio of t_{min}/t_0 decreases with decreasing viscosity. Therefore, for a coating bead governed by both the surface tension and viscous forces, it can be generally expected that the effectiveness of vacuum pressure is higher for lower viscosity. Lee et al.[31] experimentally studied the effects of viscosity and coating gap (downstream and upstream coating gaps were the same in their study) on the effectiveness of applying vacuum pressure. Based on their experimental results using silicon oil, applying bead vacuum will be less effective if the fluid viscosity is too high, and the range of the appropriate bead vacuum will be narrower if the coating gap is too large. Specifically, the vacuum pressure can efficiently reduce the wet thickness (comparing with the case without applying vacuum pressure) when the viscosity is approximately less than 500 mPa-s, the coating gap is less than 0.5 mm and the vacuum pressure is less than 800 Pa.[31]

Capillary, viscous and viscocapillary models discussed above are all based on Newtonian fluids. Based on the power law assumption for viscosity, corresponding models for non-Newtonian fluids can also be derived. Specific expressions are not discussed here, although more details have been reported.[21] It should be noted that most of the studies reviewed in this article do not differentiate the coating gap or surface tension upstream vs. downstream: i.e., $h_u=h_d$ and $\sigma_u=\sigma_d$. Thus, in the following sections, the coating gap and surface tension of upstream and downstream will not be differentiated, unless noted otherwise. Specifically, the coating gap, both upstream and downstream, is denoted by h.

Strategies for Determining Operating Limits in Numerical Studies

The analytical models of operating limits (including vacuum pressure limits, t_0 and t_{min}) discussed above are basically one-dimensional approximations. To describe the flow filed in the coating bead more accurately, solving the 2D Navier-Stokes system numerically has been conducted by some researchers. The first study was by Sartor.[34] Later, the governing equations and boundary conditions used by Sartor were used by other researchers.[2,16,28] Because operating limits always correspond to the occurrence of coating defects, which accompany instability of the coating flow, it is not trivial to determine them numerically. Critical conditions corresponding to the occurrence of instability may be determined by a linear stability analysis, as used by Gates and Scriven.[35] To predict the critical conditions of t_{min}, specifically, two strategies have been used in previous studies. The first is based on finding the turning point in a solution path that corresponds to instability of the flow field.[2,27,36] The second strategy approximate the occurrence of t_{min} as the static contact angle between the downstream meniscus and the downstream die lip becomes sufficiently small. For example, Romero et al.[16,28] used 10° as the threshold, and Bajaj et al.[37] used 20°. The basic idea of the second strategy is that t_{min} is related to extreme curvature of the downstream meniscus.[28]

Strategies for numerically determining the occurrence of t_0 and the lower limit of vacuum pressure are similar because t_0 is just a special point at the lower limit of vacuum pressure. Based on the discussion in the section titled *viscous model of operating limits*, for a viscous coating bead, t_0 at the lower limit of vacuum pressure occurs when the upstream meniscus moves close to the slot exit. The upper limit of vacuum pressure occurs when the upstream meniscus moves beyond the upstream corner of the die. Thus, in some numerical studies the position of the upstream meniscus (approaching the slot exit or the upstream corner of the die) is used as an indicator to approximately define the occurrence of t_0 at the lower limit of vacuum pressure, and the upper limit of vacuum pressure.[27,38–43] However, this strategy is only a macroscopic approximation that does not really reveal the mechanism of coating instability corresponding to t_0 at the lower limit of vacuum pressure, and the upper limit of vacuum pressure. Additionally, this strategy will be relatively inaccurate if the upstream meniscus is stretched considerably before instability appears, as shown in Figure 6 (some experimental evidence can be found in Refs. 38,44,45). Because, it will be difficult to determine the exact upstream meniscus position at which the operating limits occur.

Bhamidipati et al.[7,46,47] used another strategy to determine the occurrence of t_0. Instead of using the position of the upstream meniscus as an indicator, they calculated numerically the unsteady upstream contact line and engulfment of air bubbles inside the coated film as a direct indicator for t_0, based on both 2D and three-dimensional (3D) models. Although the studies by Bhamidipati et al.[7,46,47] focused only on highly viscous fluids, their strategy for determining the occurrence of t_0 would be expected to also be effective for cases where a surface tension effect is significant.

Two Regions of t_{min}

Based on Eq. 4, the low-flow limit t_{min} of the slot die coating process increases as capillary number increases. Defining t/h as the dimensionless wet thickness, the low-flow limit based on Eq. 4 can be plotted as curve ① in Figure 7. The area below curve ① is another form of the coating window,[2] in which a stable coating can be obtained under an appropriate vacuum pressure.

As discussed above, Eq. 4 is based on the Landau–Levich boundary condition. Thus, it is limited to small capillary and Reynolds numbers. However, practical coating conditions usually do not satisfy this assumption. Thus, it is important to assess the valid region of Eq. 4 and to study the characteristics

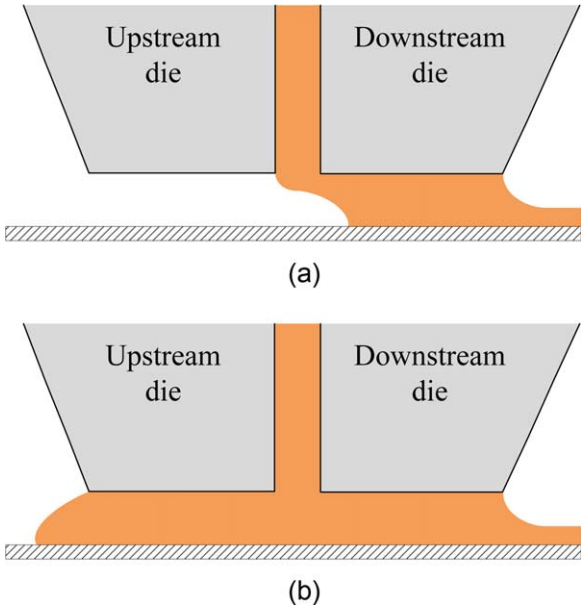

Figure 6. Schematic of the stretch of the upstream meniscus before instability appears.

(a) Upstream meniscus corresponding to t_0 or the lower limit of vacuum pressure. (b) Upstream meniscus corresponding to the upper limit of vacuum pressure. [Color figure can be viewed in the online issue, which is available at wileyonlinelibrary.com.]

of the low-flow limit outside this region. Carvalho and Kheshgi[2] studied this problem through solving a 2D Navier-Stokes system numerically for the slot coating flow and experimental validation. Based on their results, the low-flow limit can be divided into two regions: *low inertia/capillary* and *high inertia/capillary* regions. In the low inertia/capillary region, the low-flow limit is described well by Eq. 4. However, in the high inertia/capillary region, the minimum wet thickness is found to decrease as capillary number increases, which is the opposite of the trend in the low inertia/capillary region. The low-flow limit in the high inertia/capillary region is plotted as curve ② in Figure 7. Above curve ②, the coating bead is stable, while below curve ②, it is unstable. The region above curve ② is the extended coating window. The importance of Figure 7 is that for a specific coating thickness, the coating process can be conducted in the high inertia/capillary region, which can significantly increase the maximum possible coating speed restricted by the low-flow limit of the low inertia/capillary region.

Another important conclusion found by Carvalho and Kheshgi[2] is that the low-flow limit in the high inertia/capillary region is significantly affected by the vacuum pressure. Specifically, t_{min} increases as the vacuum pressure increases. This means that curve ② in Figure 7 will shift to the left at a higher vacuum pressure. This phenomenon is completely different from what has been found in the low inertia/capillary region, in which the low-flow limit is independent of vacuum pressure (Figures 2 and 5): i.e., curve ① in Figure 7 will not change when the vacuum pressure changes.

In the high inertia/capillary region, inertial forces become significant and the coating bead is mostly balanced between the inertial forces and viscous forces. Hens and Boiy[48] were the first to systematically study the effects of inertial forces in high speed slot die coating process. They explained the inertial effects in coating flow with the *boundary layer theory*. Specifically, the growth length of viscous boundary layer, L_b, on the substrate increases as inertial forces increase. Based on boundary layer theory, L_b is given by[2,48]

$$L_b = k\frac{\rho U t^2}{\mu} \tag{11}$$

where k is a coefficient. Based on classical boundary layer mechanism, k is 0.383.[48] Hens and Boiy[48] argued that L_b is the required length of coating bead to get the desired coating thickness t. Hens and Boiy[48] experimentally measured the length of the coating bead under different coating conditions. They found that Eq. 11 can satisfactorily describe the relation between U, μ, t, and L_b. However, the coefficient k was significantly different than 0.383. That is mainly because the flow conditions prevailing in the coating bead of slot die coating and the boundary layer theory are quite different.[48]

Carvalho and Kheshgi[2] further explained the low-flow limit described by curve ② by the boundary layer theory. In the high inertia/capillary region, inertial forces can push the downstream meniscus away from the coating bead, making a longer coating bead. That actually shifts the downstream meniscus away from the low-flow limit. Based on a simple geometrical argument, Carvalho and Kheshgi[2] assumed a minimum growth length, L_b^*, below which a stable 2D coating bead cannot exist. Substituting L_b^* into Eq. 11 and rearranging the equation can give the low-flow limit in the high inertia/capillary region:

$$t_{min} = \left(\frac{k\rho U}{\mu L_b^*}\right)^{-\frac{1}{2}} \tag{12}$$

It can be seen from Eq. 12 that in the high inertia/capillary region, t_{min} decreases as coating speed increases. Thus, it also decreases as capillary number increases. The relationship described by Eq. 12 has been validated preliminarily by comparing some theoretical and experimental results.[2] Equation 12 can also explain the phenomenon that t_{min} increases as the vacuum pressure increases because L_b^* is expected to be larger at a higher vacuum pressure. However, because both k and L_b^* are unknown, Eq. 12 can only qualitatively provide the effects of coating speed and viscosity on t_{min}, but cannot quantitatively predict the value of t_{min}. In addition, the boundary layer mechanism explains the transition between two regions of t_{min}, only qualitatively. In Carvalho and Kheshgi's[2] study, the critical capillary number corresponding to the transition between two regions of t_{min} varied considerably between 0.3 and 0.7. However, to our knowledge, no other systematic study of the

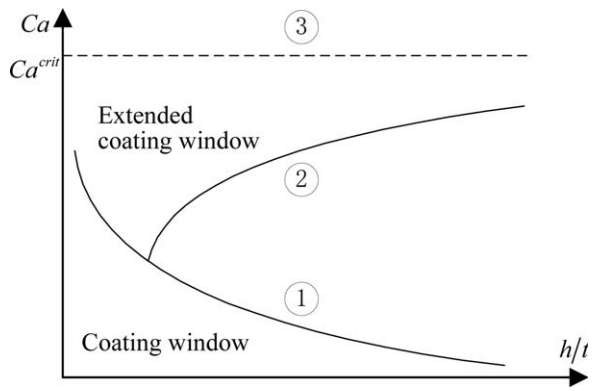

Figure 7. Extended operating region at a given vacuum pressure (recreated based on Ref. 2).

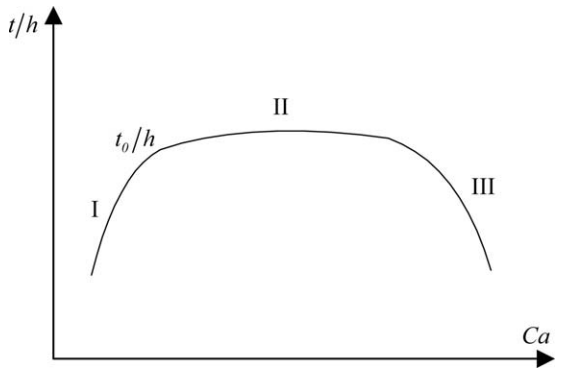

Figure 8. Three regions of t_0 in terms of *Ca* (recreated based on Refs. 28, 32).

two regions of t_{min} has been reported to reveal further the mechanism underlying this issue.

The extended coating window in the high inertia/capillary region (Figure 7) cannot be infinitely large. An upper bound must exist. Carvalho and Kheshgi[2] simply mentioned an upper bound due to the instability of the upstream meniscus of the coating bead, but with no further discussion. Although the upper bound was not clearly determined in previous studies, it actually corresponds to dynamic wetting failure, which is a common operating limit in all kinds of coating processes. This bound is indicated by the dashed line ③ in Figure 7. This bound is basically an operating limit corresponding to the maximum coating speed. It is not a limit of wet thickness. A detailed discussion of dynamic wetting failure will be given in the section titled *dynamic wetting failure*.

Three Regions of t_0

As discussed above, t_0 is an important operating limit for applications that do not use vacuum pressure. Thus, it is important to study the factors influencing t_0. Lee et al.[31] and Chang et al.[32] extensively studied the effect of capillary number on t_0 by coating Newtonian glycerin solutions and silicone oils. Based on their experimental results, there are three regions of t_0, which are shown schematically in Figure 8, in which t/h is the dimensionless wet thickness. Thus, t_0/h is the dimensionless form of the thinnest wet thickness when vacuum pressure is zero.

In region I, t_0 increases with capillary number. This phenomenon has been found in many experiments using Newtonian or approximately Newtonian fluids.[17,31,32,44,45,49,50] The capillary number is relatively small and the surface tension force (capillary pressure) is significant in this region. The trend of t_0 can be explained by the capillary or viscocapillary models of operating limits developed by Ruschak[23] and Higgins and Scriven.[25] Specifically, when the surface tension force is the only dominant force in the coating bead, the trend of t_0 in region I can be described theoretically by Eq. 5, in which t_0 increases with capillary number to the power of $2/3$: i.e.,

$$t_0 \propto Ca^{\frac{2}{3}} \tag{13}$$

The accuracy of the relationship (13) has been demonstrated experimentally in some studies.[31,44,45] When both surface tension and viscous forces are significant in the coating bead, Eq. 9 will be more accurate than Eq. 5 to describe the trend of t_0 A comparison between Eqs. 5 and 9 can be found in Lee et al.'s[31] report.

When the capillary number is sufficiently high, the effect of viscous force will be much more significant than surface tension force. In this case, the coating may enter the second region where t_0 is independent of capillary number. Although not directly determined by Lee et al.[31] or Chang et al.,[32] region II actually follows the viscous model of operating limits developed by Higgins and Scriven.[25] As given by Eq. 7, t_0 is $0.5h_d$ for a viscous coating bead. Based on many experimental results from coating Newtonian or approximately Newtonian solutions, t_0 in region II is generally between $0.5h_d$ and $0.7h_d$,[31,32,44,45,49–51] which is quite close to Eq. 7. Thus, viscous force is dominant in region II.

When the capillary number is even higher, there may be a third region where t_0 appears to decrease with capillary number. This region has been demonstrated to be governed by the inertial force,[17,32] which is similar to the high inertia/capillary region of t_{min}. Additionally, the trend in t_0 described by region III in Figure 8 is also similar to the trend of t_{min} described by curve ② in Figure 7. However, as discussed above, t_0 and t_{min} are physically different. Specifically, t_{min} corresponds to the movement of the downstream meniscus, whereas t_0 corresponds to the movement of the upstream meniscus. Thus, region III of t_0 cannot simply be explained by the boundary layer mechanism developed by Carvalho and Kheshgi.[2] To date, there is no mechanism to quantitatively explain region III of t_0. Based on Carvalho and Kheshgi's[2] explanation, the downstream meniscus is stabilized by inertial force in the high inertia/capillary region of t_{min}. Thus, it can be expected that region III of t_0 is caused by the stabilizing effect of inertial force on the upstream meniscus. Because inertial force is dominant in this region, t_0 can be correlated with Reynolds number[17,32]:

$$t_0 \propto Re^{\alpha} \tag{14}$$

Chang et al.[32] defined Re as $\rho Q/\mu$, in which ρ is the density of the coating fluid. In this definition, Re is the ratio of the fluid inertia to the viscous force at the slot exit. Based on this definition, Chang et al.[32] found α to vary between -1.5 and -2.6 in region III. In another study, Chang et al.[17] defined Re as the ratio of the fluid inertia at the slot exit to the viscous drag force on the moving substrate, i.e., $\rho U_s{}^2 h/\mu U$, in which U_s is the fluid velocity at the slot exit. Based on this definition, Chang et al.[17] found α to vary between -1.24 and -1.5 in region III. Regardless of which definition of Reynolds number is used, the value of α is apparently different from the value of -0.5 in

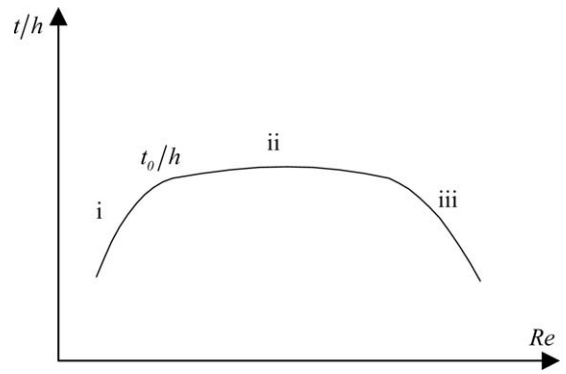

Figure 9. Three regions of t_0 in terms of *Re* (recreated based on Refs. 17, 32).

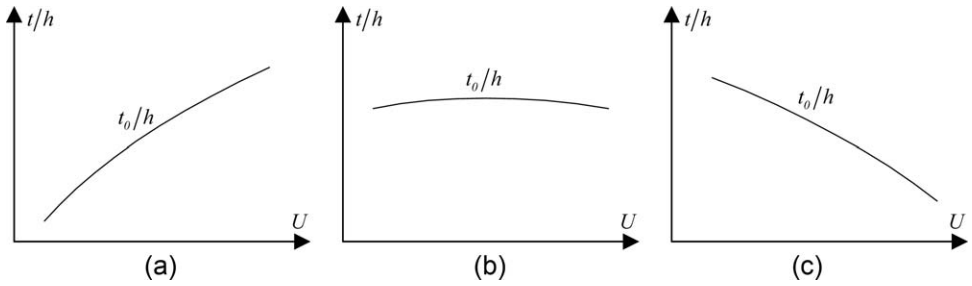

Figure 10. Three regions of t_0 in terms of governing forces.

(a) Surface tension region. (b) Viscous region. (c) Inertial region

Eq. 12. This is more evidence of a difference between the mechanisms of t_0 and t_{min}.

Based on the discussion above, t_0 decreases with Reynolds number when the inertial force is high enough to stabilize the coating bead. Generally, when the Reynolds number is relatively high, the coating speed and flow rate will be high; thus, the capillary number will be relatively high. Hence, it can be observed experimentally that t_0 decreases with capillary number when capillary number is sufficiently high,[17,32] i.e., region III in Figure 8. Because the Reynolds number is also an important factor influencing t_0, Chang et al.[32] and Chang et al.[17] plotted t_0 with Reynolds number and found there were also three regions of t_0, as shown in Figure 9. Region iii in Figure 9 corresponds to region III in Figure 8. Although only a little information can be found for regions i and ii in studies by Chang et al.[32] and Chang et al.,[17] these two regions are expected to correspond to regions I and II in Figure 8, respectively.

It can be seen from the discussion above that the regions of t_0 are determined by the competition of surface tension, viscous, and inertial forces. Thus, it is inappropriate to correlate t_0 solely with either capillary number or Reynolds number, because neither of these numbers can comprehensively represent the relative magnitude of three forces. The existence of different regions of t_0 should *not* simply be explained as *with the increase of Ca/Re, the coating will change from region I/i to region II/ii then region III/iii*. A better expression of the three regions of t_0 might be: when surface tension force dominates, t_0 increases as coating speed increases; when viscous force dominates, t_0 does not change with coating speed; and when inertial force is high enough to stabilize the coating bead, t_0 decreases as coating speed increases. These three regions are named the surface tension, viscous, and inertial regions, respectively, and are shown schematically in Figure 10.

It should be mentioned that the three regions do not necessarily appear together in real coating processes. Depending on the relative magnitude of the three forces, one, two, or all three regions may be observed. Specifically, any of the above three regions may exist alone, and any two of the three may exist together. This can be seen in many experimental results.[17,31,32,44–46,49–52] Lee et al.[31] showed experimentally that the critical capillary number corresponding to the transition of the surface tension region and the viscous region was affected significantly by the coating gap. Depending on the specific value of the coating gap, the critical capillary number in their study varied considerably, between 0.1 and 0.7. Based on the experimental results of Chang et al.[32] and Chang et al.,[17] the critical Reynolds number corresponding to the transition of the viscous region and the inertial region seems to be around 20. Another interesting finding is that although the discussion above of the regions of t_0 is based on Newtonian fluids or approximately Newtonian fluids, three regions of t_0 have also been observed in experiments with coating of non-Newtonian fluids.[44–46,49,52] However, to date, our understanding of the three coating regions of t_0 is still mostly qualitative. There is not yet a quantitative strategy to determine the existence and transitions of different regions.

All rheological and geometrical parameters that affect the force competition in the coating bead can influence t_0. Important parameters include viscosity, surface tension, coating gap, lip length, slot width, and die orientation. Viscosity and surface tension directly determine the relative strength of viscous force to surface tension force. In practice, viscous force generally dominates the coating bead for a relatively high viscosity coating fluid. In this case, t_0 is expected to be around half of the coating gap. This phenomenon can be found in some experimental studies with high-viscosity coating solutions.[46]

The coating gap is a key geometric parameter affecting t_0. Specifically, based on Eqs. 5 and 7, t_0 decreases with the coating gap (the upstream gap or downstream gap) in the surface tension and viscous regions. However, based on the experimental results of Chang et al.[32] and Chang et al.,[17] the coating gap seems to have insignificant effects on t_0 in the inertial region.[17,32] Other geometric parameters, such as die lip length, slot width, and die orientation (angle between the die slot and the substrate) can also affect t_0. However, these parameters are not explicitly included in theoretical Eqs. 5 and 7 or the empirical relationship (14); thus, their effects are typically less important than that of the coating gap. To date, studies of the effects of die lip length, slot width, and die orientation on t_0 have mostly been based on experiments, and the characteristics of their effects are still not conclusive.[17,32,53]

Coating Window in Terms of Q *vs.* U

Three regions of t_0 in Figure 10 can also be expressed in the coating window in terms of Q vs. U, as shown in Figure 11. This type of coating window can be found commonly in many reports.[17,45,46,49,51,54–58] Coating can only be operated in the window bounded by three boundaries ***a***, ***b***, and ***c***. It can be seen from Figure 11 that the minimum ratio of Q to U for a specific U always occurs on the boundary ***b***. Thus, the boundary ***b***, ranging from point 1 to point 2, actually corresponds to t_0. It also corresponds to the upper limit of coating speed for a specific flow rate. The boundary ***a*** in Figure 11 corresponds to the maximum wet thickness for a specific coating speed, or the lower limit of coating speed for a specific flow rate. For the viscous region, t_0 does not change with U. Thus, the ratio of Q to U on the boundary ***b*** is constant from point 1 to point 2, and the extension of boundary ***b*** crosses the coordinate origin, as

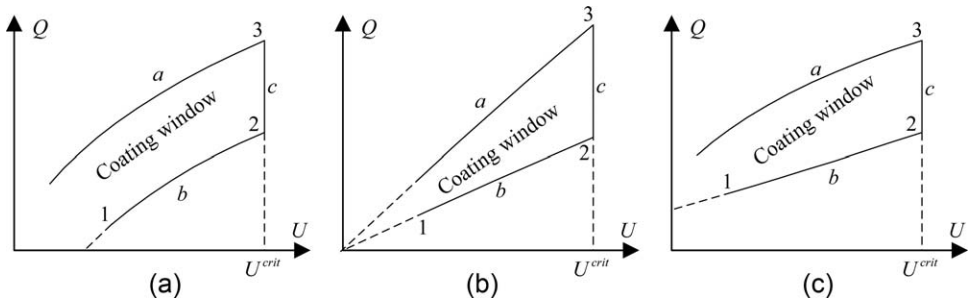

Figure 11. Schematic of coating windows in terms of *Q* vs. *U* for different regions.

(a) Surface tension region. (b) Viscous region. (c) Inertial region.

shown in Figure 11b. In addition, the expressions of boundaries ***a*** and ***b*** for the viscous region can be derived based on the viscous model of operating limits (found in the section titled *viscous model of operating limits*). Specifically, substituting $t=Q/U$ and $\Delta p=0$ into inequality (6) gives

$$\frac{2Ql_d{h_u}^2}{(l_d{h_u}^2+l_u{h_d}^2)h_d} \le U \le \frac{2Q}{h_d} \tag{15}$$

Inequality (15) is the coating speed range for a specific flow rate. The left side and right side of inequality (15) correspond to boundary ***a*** and boundary ***b*** in Figure 11b, respectively. It can be seen that the right side of inequality (15) is actually equivalent to $t_0=0.5h_d$, Eq. 7. Because inequality (15) does not include the term of viscosity, it is safe to expect that this inequality is also valid for non-Newtonian fluids. Experimental evidence for this conclusion can be found in some existing studies using relatively high non-Newtonian viscous fluids.[46]

In Figure 11, the right boundary ***c*** of the coating window corresponds to the maximum coating speed limit U^{crit}. This limit is very important because it directly determines the maximum productivity for slot die coating operations. Although it was not clearly shown in previous experimental studies,[45,49,51,54] U^{crit} actually corresponds to dynamic wetting failure, which will be discussed in the next section.

Based on the discussion in the section titled *viscous model of operating limits*, in the viscous region, the upstream meniscus on boundary ***a*** is close to the upstream corner of the die, whereas the upstream meniscus on boundary ***b*** is close to the slot exit. The upstream meniscus on boundary ***c*** can correspond to any position between the upstream corner and the slot exit, as shown in Figure 12. This can be further explained by Figure 11b. When changing the operating parameters along boundary ***c*** from point 2 to point 3 (i.e., keeping the coating speed constant and increasing the flow rate), the upstream meniscus will move from the slot exit to the upstream corner of the die. Based on elementary lubrication theory, the position of the upstream meniscus can be given approximately by

$$l_x=\left(\frac{2Q}{Uh_d}-1\right)\frac{l_d{h_u}^2}{{h_d}^2} \tag{16}$$

where l_x is the distance between the upstream meniscus and the slot exit. As will be discussed in the next section, when the coating speed exceeds the maximum wetting velocity U^{crit}, a good coating cannot be obtained regardless of the location of the upstream meniscus. This is the reason for the existence of boundary ***c***.

For the surface tension region, t_0 increases with U. Thus, the ratio of Q to U on boundary ***b*** increases from point 1 to point 2, which means the extension of boundary ***b*** crosses the axis of U, as shown in Figure 11a. For the inertial region, t_0 decreases with U. In this case, the ratio of Q to U on the boundary ***b*** decreases from point 1 to point 2; thus, the extension of boundary ***b*** crosses the axis of Q, as shown in Figure 11c. However, there are no simple analytical expressions for boundaries ***a*** and ***b*** in the surface tension and inertial regions.

Because it is generally desirable to increase the coating speed in industrial production, boundary ***a*** is practically less important than boundary ***b***. Boundary ***b***, corresponding to different regions, can be observed in many experimental results.[45,49,51,54–56] Depending on the relative magnitude of the surface tension, viscous, and inertial forces, boundary ***b*** in a real coating window may be a combination of any two or three regions in Figure 11. It should also be clarified that boundary ***c*** has been observed to be approximately vertical in some experimental studies.[45,49,50,52] Unfortunately, our understanding of the characteristics of boundary ***c*** for slot die coating is still limited. In the next section, the effects of viscosity, surface tension, and coating gap on U^{crit} will be discussed. However, to our knowledge, the effects of flow rate and die configuration on U^{crit} have not been systematically studied so far. To summarize, the coating windows in Figure 11 are illustrative and not necessarily representative, since, the coating windows can widely vary.

Dynamic Wetting Failure

Dynamic wetting is a common phenomenon, whereby the receding fluid phase on a solid surface is displaced by another advancing fluid phase. The contact line among two fluid phases and the solid is usually called the three-phase contact line or the dynamic contact line. In the slot die coating process, dynamic wetting occurs at the dynamic contact line (the contact line between the upstream meniscus and the moving substrate) where air is displaced by the coating fluid (liquid). The speed of the substrate is usually referred to as the wetting

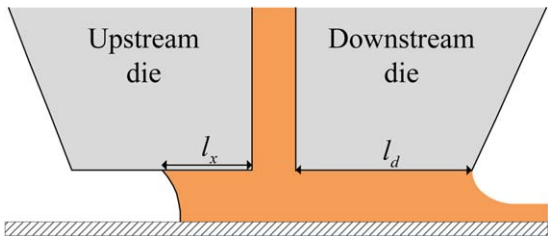

Figure 12. Position of the upstream meniscus on boundary *c*.

[Color figure can be viewed in the online issue, which is available at wileyonlinelibrary.com.]

speed. Dynamic wetting is a fundamental feature of many industrial processes, such as coating and printing. Because of its practical importance, numerous studies of dynamic wetting have been conducted over the past few decades. However, our understanding of its precise mechanism is still limited. Both macroscale (hydrodynamic) and microscale (molecular-kinetic) theories exist to explain the mechanics near the dynamic contact line. To date, the issue is still debated, as discussed in some reviews.[18,59,60] A full review of the dynamic wetting issue is beyond the scope of the current review. Here, the focus is specifically documenting related studies that are valuable for understanding dynamic wetting failure in slot die coating processes.

When the wetting speed exceeds some critical value (U^{crit}), corresponding to the critical capillary number, $Ca^{crit}=\mu U^{crit}/\sigma$, the dynamic contact line becomes unstable and breaks into a sawtooth shape.[61] This is generally referred to as dynamic wetting failure, which is often an indicator of receding fluid becoming entrained in the advancing fluid. In coating processes, this often refers to air entrainment defects and is the operating limit denoted by the dashed line ③ in Figure 7 and the boundary ***c*** in Figure 11.

Early experimental studies sought to correlate the critical coating speed with the physical properties of the coating fluid.[62–64] These studies generally agree on two things: the viscosity of the coating fluid is the most important parameter and surface tension plays a secondary role.[65] These early experimental studies were generally based on dip coating in which the meniscus near the wetting line is not confined geometrically. This is apparently different from the slot die coating process in which the upstream meniscus is confined by the die and substrate; thus, the dynamic wetting behavior may be affected significantly by such spatial restriction.

Recently, Vandre et al.[66–68] studied the effect of meniscus confinement on dynamic wetting behavior. Specifically, they investigated, experimentally and theoretically, dynamic wetting failure between two parallel plates. Although they did not use a real slot die coating system, the flow field investigated in their study was the case of an upstream bead in a slot die coating process. Thus, the results of their study are expected to be directly applicable to the slot die coating process. Their theoretical study, solving a 2D flow model, showed that wetting failure is related to an imbalance of viscous and capillary effects. Specifically, wetting failure occurs when the capillary pressure gradients, which are caused by the interface curvature, are unable to pump air away from the dynamic wetting line fast enough to maintain a steady flow.[67] Vandre et al.'s[66–68] work argues in favor of the hydrodynamic mechanism for dynamic wetting failure. Based on their experiments using glycerol/water solutions, the critical capillary number can be expressed approximately by[68]

$$Ca^{crit} \approx K\mu^{0.258} \tag{17}$$

The form of Eq. 17 looks similar to that found by other researchers for dip coating.[62,63] However, the value of K is significantly affected by confinement of the meniscus. Specifically, the value of K increases logarithmically as the coating gap decreases, thus delaying the onset of dynamic wetting failure to higher Ca^{crit}. A similar conclusion was actually experimentally obtained by Lee et al.[31] and Chang et al.,[69] which shows that the maximum coating speed (actually is the U^{crit}) increases as the coating gap decreases. This conclusion is valid only when the coating gap is smaller than the capillary length,[67] $l_{cap}=\sqrt{\sigma/\rho g}$. If the coating gap is too large, the confinement effect will be insignificant and the results will approach those found in dip coating. This conclusion clearly demonstrates that the slot die coating process is able to provide higher coating speeds than other processes without meniscus confinement, such as dip coating.

Another important conclusion that can be seen from Eq. 17 is that U^{crit} can increase significantly with a decrease in viscosity. The effect of viscosity on U^{crit} for the slot die coating process can also be seen clearly in Lee et al.'s experimental results.[31] Another interesting finding from the experiments by Vandre et al.[68] is that the vacuum pressure outside the upstream meniscus can further postpone wetting failure when the upstream meniscus is pinned at the left- or right-most corners of the upstream die.[68] When the upstream meniscus is located at some position between these two corners, a change in vacuum pressure will only shift the meniscus without changing Ca^{crit}. The study by Vandre et al.[67] also showed that Ca^{crit} increased monotonically with increasing substrate wettability (smaller static contact angle of fluid on substrate). The fluid inertia also has an apparent effect on Ca^{crit}.

Effects of Fluid Elasticity and of Adding Particles on Operating Limits

To date, existing studies on operating limits in slot die coating have been mostly based on Newtonian fluids; however, most of the fluids used in the coating industry are, in fact, polymer solutions or colloidal suspensions,[16,28] such as those used in the production of ion battery electrodes.[10,11] These fluids can represent very complex rheological properties, typically shear-thinning, extension-thickening, and viscoelastic.[28] These non-Newtonian behaviors can significantly affect the force balance in the coating bead; thus, affect the operating limits of the coating process. Thus, it is important to understand the coating characteristics of polymer solutions and colloidal suspensions.

Romero et al.[16,28] and Bajaj et al.[37] numerically studied the effects of viscoelasticity on the low flow limit (t_{min}) of the slot die coating process. In their models, only the downstream flow field was considered and the downstream meniscus was assumed to be pinned at the corner of the die. The low flow limit was approximately determined as the static contact angle between the downstream meniscus and the downstream die lip becomes sufficiently small (as discussed in the section titled *strategies for determining operating limits in numerical studies*), which is also usually called as meniscus invasion.[37] The results calculated based on different constitutive models were compared, including the algebraic model (which relates stress tensor to the rate-of-strain tensor explicitly),[28] Oldroyd-B, FENE-CR, and FENE-F models.[16,37] It was found that no matter which constitutive model was used, the fluid elasticity can generally increase t_{min}, thus destabilizing the flow near the downstream meniscus.[16,28,37] This destabilizing effect can be explained by the polymeric stress boundary layer under the downstream free surface.[16,28,37,70,71] The stress boundary layer is more sharply defined for more viscoelastic fluid. To counterbalance the pressure gradient caused by the polymeric stress boundary layer, the free surface has to curve more, thus causing meniscus invasion.

Based on experimental results, Romero et al.[28] suggested a modified capillary number for Eq. 4 to predict t_{min} more accurately for viscoelastic fluids. Specifically, the viscous term in the capillary number is replaced by the apparent extensional

viscosity. This is because the flow near the downstream meniscus for viscoelastic fluids is typically dominated by extensional deformation.

However, it has also been found that if the fluid elasticity is very small, it may stabilize the flow near the downstream meniscus, leading to a smaller t_{min} than the Newtonian case.[16] The level of fluid elasticity can be evaluated by Weissenberg number, which compares the viscous force to the elastic force. Romero et al.[16] found the critical value of Weissenberg number corresponding to the transition between the stabilizing effect and destabilizing effect to be around 0.1. Similarly, Ning et al.,[52] Yang et al.,[44] Chu et al.,[56] Huang et al.[72] have also experimentally found that low fluid elasticity can stabilize the flow near the upstream meniscus. Specifically, they found that low fluid elasticity can increase U^{crit}; however, a further increase in fluid elasticity will decrease U^{crit}. There exists an optimized level of fluid elasticity to maximize U^{cri}.[44,52,56,72] Unfortunately, the specific mechanism for the stabilizing effect of low fluid elasticity on the coating flow is still unclear. Our understanding of this stabilizing effect is still mostly qualitative.

The effects of adding particles to the coating fluid have also been studied by some researchers. Existing studies on this topic mainly concerned the stability of dynamic contact line, i.e., the maximum wetting velocity. Based on classical hydrodynamic theories, the viscosity of a dilute suspension should increase with the volume of adding particles.[73] Then, following Eq. 17, it can be expected that the maximum wetting velocity for suspensions, U_p^{crit}, will decrease with the volume of adding particles (caused by the increase of viscosity). However, in contrast, existing experimental studies have confirmed that adding particles to the coating fluid can significantly postpone the onset of dynamic wetting failure, i.e., increase the maximum wetting velocity.[45,49,51,74] This means that the effect of adding particles to the coating fluid cannot be simply explained by the change of bulk rheological properties.

Yamamura et al.[74] conducted a systematic study on the effect of particle number density to U_p^{crit}. They experimentally found that there exists a critical particle number density that can maximize U_p^{crit}. They proposed a film splitting mechanism to explain the function of particles during dynamic wetting. Based on their theory, particles can split the thin air sheet near the dynamic contact line, generating air fingers. At relatively low particle number densities, air fingers will shrink (moves toward the upstream direction). As a result, the dynamic contact line is pulled upstream, leading to a higher U_p^{crit}. At relatively high particle number densities, air fingers will break up into fine bubbles, leading to a smaller U_p^{crit}.

Based on elementary lubrication theory and their film splitting mechanism, Yamamura et al.[74] also established an analytical model to predict U_p^{crit}. Their model can qualitatively explain the relationship between the particle number density and U_p^{crit}, but fails to predict the maximum value of U_p^{crit}. Specifically, the maximum U_p^{crit} obtained from Yamamura et al.'s model is only a function of capillary number. This opposes their experimental observations whereby the maximum possible value of U_p^{crit} is also affected by particle size. In addition, Yamanura et al.[74] also showed that the maximum U_p^{crit} obtained based on their model was one order of magnitude higher than the experimental results. Therefore, the film splitting mechanism proposed by Yamamura et al., only partially explains the effect of particles on the dynamic wetting. Hence, more work is needed to obtain a basic understanding of the mechanisms underlying this issue.

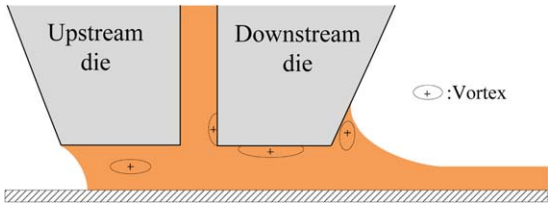

Figure 13. Vortices in slot die coating flow.

[Color figure can be viewed in the online issue, which is available at wileyonlinelibrary.com.]

Chu et al.[45] explained the effect of particles on U_p^{crit} from another perspective. Based on their experimental results, the porous particles can lead to a larger U_p^{crit} compared with the hard particles with the same size. Therefore, U_p^{crit} is strongly dependent on the total surface area of particles. Based on Chu et al.'s[45] explanation, larger surface area of particles can cause more attachment points for polymer chains, thus stronger inter-particle bridging, which leads to an increase in the local and total surface tension. Chu et al.[45] believed that surface tension can stabilize the coating flow, thus increase U_p^{crit}. The stabilizing effect of surface tension on the dynamic wetting line can be partially explained by Eq. 17, which shows the maximum wetting velocity linearly increases with surface tension. However, in Chu et al.'s[45] experiments, a 16% increase in surface tension can cause a 50% increase in U_p^{crit}. It seems that the stabilizing effect of surface tension in suspensions is stronger than that in pure solutions without particles. Chu et al.[49] further explained that the flow stability is promoted not only by the surface tension, but also the amount of polymer adsorption which determines the steric forces surrounding particles. However this explanation is still vague and does not completely reveal the mechanism of particle effects on dynamic wetting.

Vortex-Free Operating Window

Various numerical and experimental studies have found that vortices may appear in the coating flow even if the operation is conducted in the operating window bounded by regular operating limits, including the vacuum pressure limits, low-flow limit, and dynamic wetting limit.[29,34,36,40,41,75] Vortices may appear inside the feed slot,[34,42] under the die lip,[34] or near the downstream contact line,[40] as shown in Figure 13. The operating region in the parameter space without vortices has been named the vortex-free operating window,[41,42,75] which is bounded by operating conditions for the onset of a vortex. Based on prior studies,[41,42,76] the area of the vortex-free operating window is usually much smaller than that of the operating window bounded by regular operating limits. Vortices in the coating flow may cause several undesired coating defects,[42,75] especially for a slurry or highly concentrated suspension coating fluid.[41] Thus, it is meaningful to predict the vortex-free operating window for slot die coating operations.

The discussion of operating limits in previous sections was based mainly on the standard/uniform die lip (as shown in Figures 1 and 3). However, in practice, die lip configurations may be much more complex, as shown in Figure 14. Some numerical and experimental studies have been conducted to study the effects of slot die lip configuration on vortex generation in the coating bead.[29,34,36,40–42,77] Based on the results of these

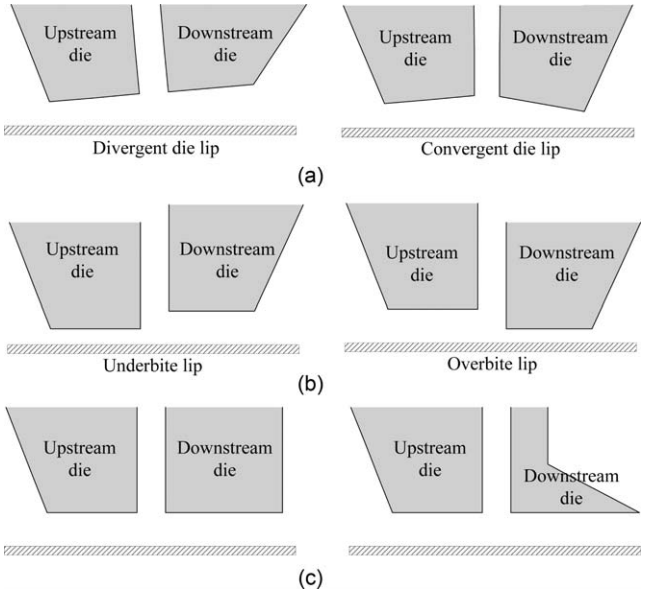

Figure 14. Different die lip configurations: (a) die lips with different slope angles, (b) die lips with different relative magnitude of coating gaps, and (c) die lips with different downstream shoulder angles.

Other lip configurations with complex angles or shapes can be found elsewhere.[27,30,41]

studies, vortex generation in the coating bead is affected significantly by several geometric parameters of die lips, including the sloped angle of die lips (as shown in Figure 14a), the relative magnitude of coating gaps (as shown in Figure 14b), and the downstream shoulder angle (as shown in Figure 14c). Sartor[34] and Nam[42] found that a vortex tended to appear in the feed slot when the coating gap was approximately five times the wet thickness. Because the die lip configuration affects the flow instability in the coating bead decisively, appropriate design of the die lip can extend the vortex-free coating window. Unfortunately, there is no simple way to optimize the die lip configuration. The effects of different geometric parameters on vortex generation have to be solved numerically or observed experimentally, and the effects are still not fully understood.

Pinning of the Downstream Meniscus

In previous analytical discussions[23,25] (capillary, viscous, and viscocapillary models) and many numerical studies,[2,16,27,28,37,39,57,78–80] the downstream meniscus is assumed to be pinned at the outer corner of the downstream die. However, this assumption is not necessarily true for practical processes. As observed in many experimental studies,[17,32,38,44,45,55,58,69,81] the downstream meniscus may be located on the downstream die shoulder or at the bottom of the downstream die lip. If the downstream meniscus is not pinned at the die corner, the accuracy of analytical models of operating limits (capillary, viscous, and viscocapillary models discussed above) will be affected negatively. Chang et al.[32] found experimentally that the position of the downstream meniscus is highly related with the region of t_0. However, to our knowledge, there is no reported systematic study revealing the effects of downstream meniscus location on the accuracy of the analytical models of operating limits.

If the downstream meniscus is located on the die shoulder, the flow field near the meniscus tends to form a vortex.[36,40] Dry residuals may accumulate on the die shoulder, which may be dragged into the coating fluid periodically and impair the coating quality.[40] Some numerical and experimental work has been conducted to study the effect of die lip configuration on the pinning of the downstream meniscus. Romero et al.[36] argued that the downstream edge was actually a rounded corner due to the limitations of the machining process. They studied numerically the effects of the radius of the corner on the mobility of the downstream meniscus and found that minimizing the radius of the corner is necessary to apparently pin the downstream meniscus. Lin et al.[40] determined that proper design of the downstream die shoulder angle (as shown in Figure 14c), the hydrophobicity of the die surface, and the coating gap can help pin the downstream meniscus. Sartor[34] also argued that proper control of the liquid contact angle and wet thickness and the use of a sharp die corner can help to pin the downstream meniscus. However, to date, the precise mechanism determining the downstream meniscus location remains unclear.

Operating Limits in the Tensioned-Web-Over-Slot Die Coating Process

So far, our discussion in this review has been based on the conventional fixed-gap slot die coating process, in which the substrate is usually supported by a rigid back-up roll, as shown in Figure 15. The coating gap in conventional slot die coating is controlled by mechanical settings. As discussed in previous sections and given by Eqs. 4, 5, 7, and 9, the thinnest possible wet thickness (with/without use of vacuum pressure), t_{min} and t_0, that can be obtained by conventional slot die coating are significantly affected by the coating gap. Thus, ultrathin films can be obtained only by adjusting the coating gap to a very small value. However, due to the effects of machining errors, assembly errors, and mechanical vibration, the conventional slot die coating process suffers the risk of the roll and the die clashing if the coating gap is too small. It is very difficult to control the wet thickness to be smaller than 15 μm in real industrial applications.[4,5] This is a significant practical limitation to the thinnest possible wet thickness (with/without use of vacuum pressure) that can be obtained by the conventional slot die coating process.

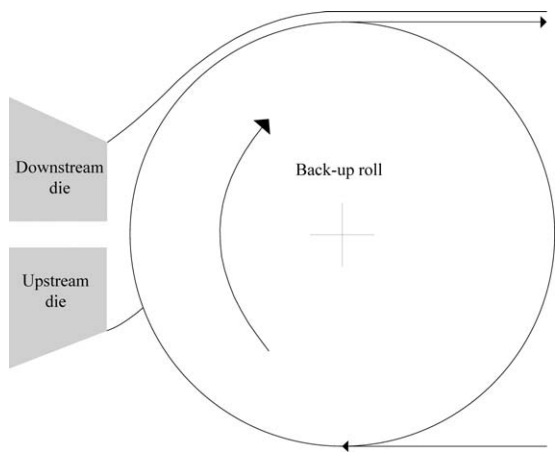

Figure 15. Schematic of a traditional fixed-gap slot die coating system.

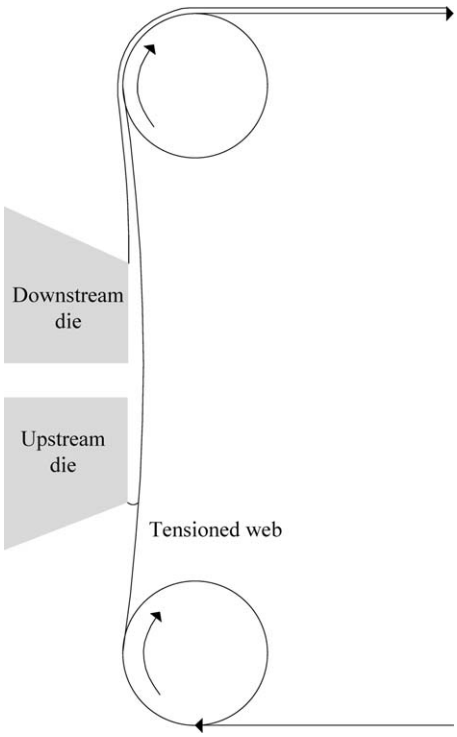

Figure 16. Schematic of a TWOSD coating system.

To overcome the limitations of the traditional slot die coating process, the TWOSD coating method has been introduced. As shown in Figure 16, instead of using a rigid distance between the backup roll and the coating die, the TWOSD coating process has a flexible coating gap which can avoid clashing with the die lip. The coating gap is determined by an *elastohydrodynamic* interaction, which is the interaction between the hydrodynamic force of the liquid flow and the tensional force of the substrate. Generally, the TWOSD coating method can easily maintain an extremely small coating gap, up to a few microns,[42,76] which makes it an important method for coating ultrathin films, such as optical films.[4,5] Another advantage of the TWOSD coating process is that there is no need for a vacuum pressure to stabilize the coating bead.[42]

Due to its apparent importance for the coating industry, many patents for TWOSD coating methods have been issued, as summarized by Lin et al.[4,5] However, only a few studies can be found in the literature on the operating limits of TWOSD coating processes. Our understanding of the fundamentals of this coating method is still limited. The flow of TWOSD coating is much more complex than that of the traditional slot die coating process because the coating gap is a variable, since it is determined by an elastohydrodynamic interaction. Solving such a flow field requires coupling of the governing equations of the coating bead and the equations describing the substrate deformation, which is not trivial for obtaining analytical solutions. Thus, the operating limits of the TWOSD coating process cannot be expressed simply by explicit expressions, such as the operating limit models (Eqs. 4, 5, 7, and 9) for conventional slot die coating.

The first theoretical study of the flow of TWOSD coating was reported by Feng[82] who solved the coupling of 2D Navier-Stokes equation and membrane theory by a finite element method. However, Feng[82] focused mainly on the elastohydrodynamic effects in the TWOSD coating process, and did not study the operating limits of the process. Later, Park[83] built an elasto-visco-capillary model to describe the flow of TWOSD coating. This model is a 1D approximation that determines the coating window by means of the upstream meniscus. Lin et al.[5] studied the effects of viscosity, web tension, and die configuration on the coating window and the "minimum wet thickness" of a TWOSD coating process, experimentally. Vacuum pressure is generally not used in TWOSD coating, and the coating window studied by Lin et al.[5] was the relationship between Q and U under atmospheric conditions (as shown in Figure 11), and the "minimum wet thickness" was t_0. Lin et al.[4] also built a 1D macroscopic model to predict t_0. This model is based on the coupling of lubrication theory and simplified membrane theory. Lin et al.[5] determined t_0 by searching for the turning point on a solution path. Their theoretical predictions reasonably followed the same trends as their experimental results.[4,5] Although Park[83] and Lin et al.'s[4] 1D models are relatively less computationally expensive, the process for building and solving such models are not simple. In addition, both models require complex numerical calculation strategies, and cannot provide information on vortices in the flow.

Nam and Carvalho[42] built a 2D model to study the operating limits of TWOSD coating flow. That model couples the 2D Navier-Stokes equation and thin inextensible shell theory, and assumes that the downstream meniscus is pinned at the outer corner of the downstream die lip. Nam and Carvalho[42] determined coating window and t_0 by means of the position of the upstream meniscus, and determined the vortex-free coating window using an automatic tracking method of vortex.[75] Lin et al.[5] and Nam et al.'s[76] experiments on TWOSD coating also demonstrated that t_0 occurs when the upstream meniscus is close to the slot exit. By means of a 2D theoretical model, Nam and Carvalho[42] studied the effects of several geometric parameters (including die lip length, die lip curvature, downstream apex point, and straight die lip) on the coating window, the vortex-free coating window, and t_0. Nam et al.[76] demonstrated the accuracy of their theoretical predictions of the coating window and the vortex-free coating window, experimentally. The coating window (or vortex-free coating window) in the studies by Nam et al.[42,76] is the relationship between the wet thickness and the tension number. Tension number T_N is defined as $\mu U/T$, where T is the tension of the substrate. Tension number is a direct function of U, whereas wet thickness is a direct function of Q, so the coating window (or vortex-free coating window) studied by Nam et al.[42,76] basically represents the relationship between Q and U (as shown in Figure 11). Based on some existing theoretical and experimental studies,[5,42] the relationship between t_0 and the tension number is given by[5,42]

$$t_0 = C T_N{}^m \tag{18}$$

In existing studies,[5,42] m is usually found to be around 0.5 (which is not absolutely accurate because m also depends on the die configuration[42]). C is a function of geometric and rheological parameters. Lin et al.[5] expressed C as a function of two dimensionless groups (pressure number and dimensionless capillary length). Nam et al.[42] expressed C as a function of die lip curvature. Overall, the specific expressions of Eq. 18 given by Lin et al.[5] and Nam et al.[42] are based only on limited experimental observations or numerical simulations. Their accuracy has not been broadly demonstrated. Based on existing

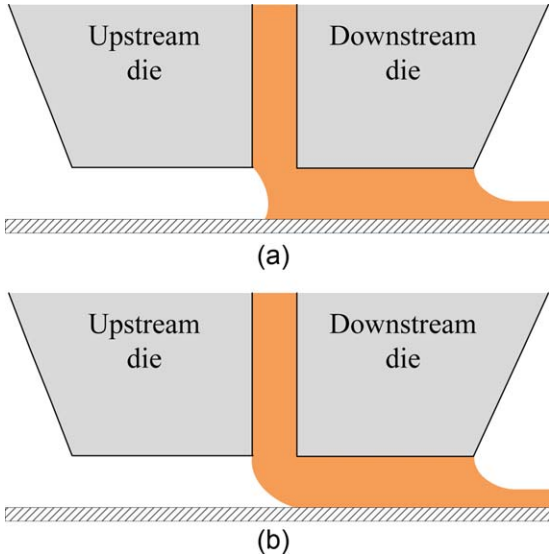

Figure 17. Schematic of concave and convex upstream menisci.

(a) Concave. (b) Convex. [Color figure can be viewed in the online issue, which is available at wileyonlinelibrary.com.]

studies,[4,5,42,76,83] the operating limits of the TWOSD coating process are also affected significantly by the die lip configuration. However, due to the variety of shapes and geometries of die lips, it is hard to provide any conclusive discussion on the effects of different die lip configurations. An efficient and effective model to predict the coating window and t_0 of TWOSD should involve some explicit expressions (like Eqs. 4, 5, 7, and 9), and not require solving complex differential equations. Unfortunately, due to the complexity underlying this problem, this model does not currently exist.

A Brief Discussion on Coating Defects Related to Operating Limits

Coating defects are an issue closely related with operating limits. Several types of coating defects related with slot die coating can be found in existing studies, such as dripping, ribbing, air entrainment, and rivulets. Many experimental results for coating defects have been reported. However, it is not trivial to provide a summary of this issue, because different coating defects are caused by different mechanisms, and the precise mechanisms of most types of coating defects are still unclear. A full review of coating defects is beyond the scope of the current review. The focus in this section is to pick the most common defects in the slot die coating process based on experimental results in the literature, and to correlate these defects with different operating limits.

The typical coating defect corresponding to t_{min} is ribbing.[15] Ribbing is a periodic thickness variation in the cross-web direction. It is a 3D flow instability that occurs when the viscous force is too high to be balanced by the capillary force of the downstream meniscus. In this case, the coating bead tries to compensate for the viscous pressure drop through the nonuniform curvature of the downstream meniscus in the cross-web direction.[15] Ribbing will transform into rivulets (alternating uncoated and coated stripes) if the pressure difference between upstream and downstream menisci is too high to be held by the coating bead.[2,28]

Experimental observations of coating defects related to the limit of dynamic wetting failure can also be found in some studies.[45,49,51] Based on the discussion in the section titled *dynamic wetting failure*, the defect corresponding to this limit is air entrainment (typically means air bubbles trapped within the coated film), caused by the maximum wetting velocity. However, rivulets are also usually observed. Based on the observations of Chu et al.,[45] the rivulets are caused by large-scale air entrainment.

The coating defects related to the operating limit of t_0 have been extensively studied by Liu and coworkers.[5,17,31,32,38,44,45,49,51,52,54–56,58,72] Based on their experimental results, the typical defects related to t_0 are cross-web periodic thickness variation[52,54] and air bubbles trapped within the coated film.[45,52] The cross-web periodic thickness variation on the limit of t_0 is usually observed in low-viscosity and low-capillary-number situations[17,31,44,51]; whereas the air bubbles on the limit of t_0 are usually observed in high-viscosity and high-capillary-number situations.[17,31,44,51] In addition, some studies[32,38,44] have shown that the cross-web periodic thickness variation on the limit of t_0 corresponds to a concave upstream meniscus with a dynamic contact angle smaller than 90°, as shown in Figure 17a; whereas air bubbles on the limit of t_0 corresponds to a convex upstream meniscus with a dynamic contact angle close to 180°, as shown in Figure 17b.

It can be seen that the phenomenon of the cross-web periodic thickness variation on the limit of t_0 looks the same as traditional ribbing defect observed on the limit of t_{min}. Therefore, it is also called "ribbing" in many existing reports. However, it has to be clarified that the cross-web periodic thickness variation on the limit of t_0 is fundamentally different from traditional ribbing defect on the limit of t_{min}. Specifically, the traditional ribbing defect is related to the instability of the downstream meniscus; whereas, the cross-web periodic thickness variation on the limit of t_0 is related with the upstream instability. Based on the experimental results of Chang et al.,[32] when the cross-web periodic thickness variation occurs on the limit of t_0, the static contact angle between the downstream meniscus and the die lip can vary from 40° to 108°. This is apparently different from what is observed for traditional ribbing defect, for which the contact angle between the downstream meniscus and the die lip should be sufficiently small (such as 10° according to some existing studies[16,28]).

It can also be noticed that the phenomenon of air bubbles on the limit of t_0 looks similar to traditional air entrainment that is related to the limit of dynamic wetting failure. However, it should be noted that the mechanisms of air bubbles on the limit of t_0 and traditional air entrainment are different. When coating is operating close to the limit of t_0, the upstream meniscus is usually close to the slot exit. Due to geometric restriction, the upstream meniscus cannot move further downstream. In that case, a further increase in the coating speed will cause instability in the upstream meniscus leading to air bubbles. Thus, a geometric restriction on the movement of the upstream meniscus is a major factor affecting the generation of air bubbles at the limit of t_0. However, air entrainment corresponding to dynamic wetting failure is solely because the wetting velocity exceeds its maximum limit. As shown in Figure 12, the upstream meniscus, corresponding to dynamic wetting failure, can move freely at the operating limit.

At the lower limit of coating speed for a specific flow rate (boundary ***a*** in Figure 11), coating fluid is typically close to

Table 1. Summary of Operating Limits in Slot Die Coating Processes

Operating limits	Decisive meniscus	Related models	Common defects
Limits of vacuum pressure	Upstream meniscus	Inequalities (1), (6), (8), and (10)	–
Low flow limit t_{min}	Downstream meniscus	Equations 4 and 12	Ribbing, rivulets
Limit of t_0	Upstream meniscus	Equations 5, 7, 9, and 18; Relationship (13) and (14)	Cross-web periodic thickness variation, air bubbles
Limit of dynamic wetting failure	Upstream meniscus	Equation 17	Air entrainment, rivulets
Limits of coating speed for a specific flow rate	Upstream meniscus	Inequality (15)	Lower bound: dripping; Upper bound: the same as the case of limit of t_0

the upstream corner of the die. A further decrease in the coating speed will cause fluid collection behind the upstream die. In the traditional fixed-gap slot die coating process, the accumulated fluid behind the upstream die drips down along the roller. This defect is called dripping in many experimental studies.[5,38,45,49,52,55,56,58,72]

Summary of Operating Limits in Slot Die Coating Processes

In previous sections, we have reviewed the operating limits in the slot die coating processes, including the limits of vacuum pressure, the low flow limit t_{min}, the limit of t_0, the limit of dynamic wetting failure, and the limits of coating speed for a specific flow rate. For convenience, important information related to these operating limits is summarized in Table 1.

Future Directions

Although slot die coating has been used successfully in industry for several decades, our understanding of the fundamental mechanisms underlying this process is still limited. Based on the discussion above of existing theories and experimental results, we think more research efforts should be given to the following important aspects in the future.

Mechanism of inertial effects

Inertial forces affect both t_{min} and t_0 significantly. Inertial forces have been demonstrated to be able to stabilize the coating flow, thus facilitating the process to fabricate thinner films and extend the window of operating parameters. However, our explanation of inertial effects on t_{min} and t_0 is limited only to the boundary layer mechanism (Eq. 11) and the simple empirical relationship (14) obtained from limited experimental data. Thus, more studies are required to understand the precise mechanisms of the inertial effects in coating flow.[84] This is necessary for optimizing the die configuration and operating conditions.

Predicting the existence and transition of different coating regions

Existing studies have shown that there are three regions of t_0 and two regions of t_{min}. However, our understanding of coating regions is still incomplete. As we have shown, the three regions of t_0 are dominated by surface tension, viscous, and inertial forces. The two regions of t_{min} are dominated by surface tension and inertial forces. Although there has yet to be any direct evidence, it is believed that there is also a viscous region for t_{min}. Thus, more studies regarding the characteristics of the different regions of t_{min} are needed. More importantly, we need a method to predict quantitatively the existence of each region and the transition among different regions. This is important for selecting proper operating conditions in real production scenarios.

Effects of geometric parameters of the slot die on operating limits

Die configuration plays an important role in operating limits. Based on analytical and empirical models, we know a lot about the effects of coating gap on different operating limits. However, the effects of other geometric parameters on coating flow and operating limits are still inconclusive. Common geometric parameters include die lip length, slot width, sloped angle of die lips, and shoulder angle. More work is desirable on these issues because they have significant practical importance in guiding the design of slot dies.

Mechanisms underlying various coating defects

The accuracy of predicting operating limits basically depends on whether we can precisely predict the generation of coating defects. Unfortunately, we know little about the generation mechanisms of various coating defects, such as ribbing and air entrainment. So far, the prediction of operating limits has been based largely on approximate geometric argument, such as the position of the upstream meniscus (for predicting t_0) and the angle between the downstream meniscus and the downstream die lip (for predicting t_{min}). Much work still needs to be done to determine the precise mechanisms underlying various coating defects.

Refining computational studies

In recent years, computational studies of slot die coating flow based on computational fluid dynamics (CFD) models have attracted more attention. CFD models can help to reveal the characteristics of the flow field near the dynamic contact line, which is key to understanding the mechanisms of coating defects. However, there are still no complete physical equations describing the dynamic wetting behavior. This lessens the validity of CFD calculations. Thus, research progress on the mechanism of dynamic wetting is highly desirable for further computational studies of slot die coating processes.

In addition, current CFD models are mostly 2D and do not precisely describe the 3D instability that occurs in coating flow. Recently, Bhamidipati et al.[85] conducted a 3D transient analysis of the slot die coating flow using volume-of-fluid model, and observed 3D air bubbles entrapped at the upstream meniscus when the coating speed is high enough (boundary ***b*** in Figure 11). Thus, it is possible to study the flow instability and operating limits using 3D numerical strategies. However, Bhamidipati et al.'s[47,85] 3D work was limited to a relatively coarse mesh (the finest mesh was around 50 μm), and an arbitrary assumption of parameters for the slip boundary

condition. More refined computational work in 3D space needs to be conducted in the future.

Effects of complex rheological properties and adding particles on operating limits

So far, existing studies on coating flows have been mostly based on Newtonian fluids. However, most of the fluids used in the coating industry are complex fluids, such as polymer solutions and colloidal suspensions. These fluids can represent very complex rheological properties, such as shear-thinning, extension-thickening, viscoelasticity, viscoplasticity, among others. Our understanding of the effects of complex rheological properties and adding particles on operating limits of slot die coating (or other coating methods) is still very limited. It is very hard to extract general and valuable conclusions from limited numerical and experimental data. This sets an apparent barrier for industrial practitioners to optimize operating conditions in terms of production rate and product quality. In the future, more analytical and numerical work is highly desired in this area.

Notation

C = coefficient in the expression of t_0 in terms of the tension number
Ca = capillary number
Ca^{crit} = critical capillary number corresponding to the maximum wetting velocity
h_u = upstream coating gap
h_d = downstream coating gap
k = coefficient in the expression of boundary layer theory
K = coefficient in the expression of the critical capillary number corresponding to the maximum wetting velocity
l_u = lip length of the bottom surface of the upstream die
l_d = lip length of the bottom surface of the downstream die
l_x = distance between the upstream meniscus and the slot exit
l_{cap} = capillary length
m = exponent in the expression of t_0 in terms of the tension number
Δp = vacuum pressure between the upstream and downstream menisci
Δp_t = pressure outside the downstream meniscus minus the pressure inside the downstream meniscus
Q = 2D Flow rate
Re = Reynolds number
t = wet thickness
t_{min} = the minimum wet thickness
t_0 = the thinnest wet thickness when vacuum pressure is zero
T_N = tension number
U = coating speed
U_s = fluid velocity at the slot exit
U^{crit} = the maximum wetting velocity
U_p^{crit} = the maximum wetting velocity for suspensions
w = slot width
L_b = growth length of viscous boundary layer on the substrate
L_b^* = the minimum value of L_b
$\boldsymbol{a}$, $\boldsymbol{b}$, $\boldsymbol{c}$ = labels of boundaries in the coating window in terms of Q vs. U

Greek Letters

α = exponent in the expression of t_0 in terms of Reynolds number
ρ = density of the coating fluid
μ = viscosity of the coating fluid
σ = surface tension
σ_u = surface tension at the upstream meniscus
σ_d = surface tension at the downstream meniscus
θ = dynamic contact angle
θ_s = static contact angle between the upstream meniscus and the die lip surface

Acknowledgment

This work was supported by the Beijing Institute of Technology Research Fund Program for Young Scholars and the National Science Foundation under grant number CMMI-095339.

Literature Cited

1. Beguin AE, Inventor. Method of coating strip material. US patent No. 2,681,6941954.
2. Carvalho MS, Kheshgi HS. Low-flow limit in slot coating: theory and experiments. *AIChE J*. 2000;46(10):1907–1917.
3. Tanwar J, Vinjamur M, Scriven LE. Design principles of integrated vacuum slot arrangement. *AIChE J*. 2007;53(3):572–578.
4. Lin F-H, Liu C-M, Liu T-J, Wu P-Y. A macroscopic mathematical model for tensioned-web slot coating. *Polym Eng Sci*. 2008;48(2): 307–315.
5. Lin F-H, Liu C-M, Liu T-J, Wu P-Y. Experimental study on tensioned-web slot coating. *Polym Eng Sci*. 2007;47(6):841–851.
6. Ding X, Didari S, Fuller TF, Harris TAL. Membrane electrode assembly fabrication process for directly coating catalyzed gas diffusion layers. *J Electrochem Soc*. 2012;159:B746–B753.
7. Bhamidipati KL, Harris TAL. Numerical simulation of a high temperature polymer electrolyte membrane fabrication process. *J Fuel Cell Sci Technol*. 2010;7(6):061005 (061007 pp.).
8. Krebs FC, Tromholt T, Jorgensen M. Upscaling of polymer solar cell fabrication using full roll-to-roll processing. *Nanoscale* 2010; 2(6):873–886.
9. Larsen-Olsen TT, Andreasen B, Andersen TR, Bottiger APL, Bundgaard E, Norrman K, Andreasen JW, Jrgensen M, Krebs FC. Simultaneous multilayer formation of the polymer solar cell stack using roll-to-roll double slot-die coating from water. *Sol Energy Mater Sol Cells* 2012;97:22–27.
10. Schmitt M, Baunach M, Wengeler L, Peters K, Junges P, Scharfer P, Schabel W. Slot-die processing of lithium-ion battery electrodes—coating window characterization. *Chem Eng Process* 2013;68:32–37.
11. Schmitt M, Scharfer P, Schabel W. Slot die coating of lithium-ion battery electrodes: investigations on edge effect issues for stripe and pattern coatings. *J Coating Tech Res*. 2014;11(1):57–63.
12. Sandström A, Dam HF, Krebs FC, Edman L. Ambient fabrication of flexible and large-area organic light-emitting devices using slot-die coating. *Nat Commun*. 2012;3:1002.
13. Søndergaard RR, Hösel M, Krebs FC. Roll-to-roll fabrication of large area functional organic materials. *J Polym Sci Part B Polym Phys*. 2013;51(1):16–34.
14. Gutoff EB, Cohen ED. *Coating and Drying Defects: Troubleshooting Operating Problems*. New York: John Wiley & Sons, 2006.
15. Schweizer PM, Kistler SF. *Liquid Film Coating: Scientific Principles and Their Technological Implications*. London: Chapman & Hall, 1997.
16. Romero OJ, Scriven LE, Carvalho MS. Slot coating of mildly viscoelastic liquids. *J Non-Newton Fluid*. 2006;138:63–75.
17. Chang H-M, Chang Y-R, Lin C-F, Liu T-J. Comparison of vertical and horizontal slot die coatings. *Polym Eng Sci*. 2007;47:1927–1936.
18. Blake TD. The physics of moving wetting lines. *J Colloid Interface Sci*. 2006;299(1):1–13.
19. Nam J, Carvalho MS. Two-layer tensioned-web-over-slot die coating: effect of operating conditions on coating window. *Chem Eng Sci*. 2010;65:4065–4079.
20. Nam J, Carvalho MS. Two-layer tensioned-web-over-slot die coating: effect of die lip geometry. *Chem Eng Sci*. 2010;65(13):4014–4026.
21. Schmitt M, Raupp S, Wagner D, Scharfer P, Schabel W. Analytical determination of process windows for bilayer slot die coating. *J Coating Tech Res*. 2015:1–11.
22. Brown OD, Maier GW, Inventors. Die coating method and apparatus. US patent No. 5,639,3051997.
23. Ruschak KJ. Limiting flow in a pre-metered coating device. *Chem Eng Sci*. 1976;31(11):1057–1060.
24. Landau L, Levich B. Dragging of a liquid by a moving plate. *Acta Physicochim URSS* 1942;17:42–54.
25. Higgins BG, Scriven LE. Capillary pressure and viscous pressure drop set bounds on coating bead operability. *Chem Eng Sci*. 1980; 35(3):673–682.
26. Ruschak KJ. Coating flows. *Annu Rev Fluid Mech*. 1985;17:65–89.
27. Quinones DM, Carvalho MS. Effect of die lip configuration on the operating window of slot coating process. Paper presented at: 11th Brazilian Congress of Thermal Science and Engineering (ENCIT 2006), Curitiba, 2006.
28. Romero OJ, Suszynski WJ, Scriven LE, Carvalho MS. Low-flow limit in slot coating of dilute solutions of high molecular weight polymer. *J Non-Newton Fluid* 2004;118:137–156.
29. Gates ID. *Slot coating flows: feasibility, quality* [Ph.D. dissertation], University of Minnesota, 1999.

30. Youn SI, Kim SY, Shin DM, Lee JS, Jung HW, Hyun JC. A review on viscocapillary models of pre-metered coating flows. *Korea-Aust Rheol J*. 2006;18(4):209–215.
31. Lee K-Y, Liu L-D, Liu T-J. Minimum wet thickness in extrusion slot coating. *Chem Eng Sci*. 1992;47:1703–1713.
32. Chang Y-R, Chang H-M, Lin C-F, Liu T-J, Wu P-Y. Three minimum wet thickness regions of slot die coating. *J Colloid Interface Sci*. 2007;308:222–230.
33. Bhamidipati KL, Didari S, Harris TAL. Experimental study on air entrainment in slot die coating of high-viscosity, shear-thinning fluids. *Chem Eng Sci*. 2012;80:195–204.
34. Sartor L. *Slot coating: fluid mechanics and die design* [Ph.D. dissertation], University of Minnesota, 1990.
35. Gates ID, Scriven LE. Stability analysis of slot coating flows. Paper presented at: AIChE Meeting, New Orleans, LA, 1996.
36. Romero OJ, Scriven LE, Carvalho MS. Effect of curvature of coating die edges on the pinning of contact line. *AIChE J*. 2006;52(2):447–455.
37. Bajaj M, Prakash JR, Pasquali M. A computational study of the effect of viscoelasticity on slot coating flow of dilute polymer solutions. *J Non-Newton Fluid*. 2008;149(1–3):104–123.
38. Lin C-F, Wong DSH, Liu T-J, Wu P-Y. Operating windows of slot die coating: comparison of theoretical predictions with experimental observations. *Adv Polym Tech*. 2010;29(1):31–44.
39. Lee SH, Koh HJ, Ryu BK, Kim SJ, Jung HW, Hyun JC. Operability coating windows and frequency response in slot coatings flows from a viscocapillary model. *Chem Eng Sci*. 2011;66:4953–4959.
40. Lin C-F, Wang B-K, Tiu C, Liu T-J. On the pinning of downstream meniscus for slot die coating. *Adv Polym Tech*. 2013;32(S1):E249–E257.
41. Lee S, Kim S, Nam J, Jung H, Hyun J. Effect of sloped die lip geometry on the operability window in slot coating flows using viscocapillary and two-dimensional models. *J Coating Tech Res*. 2014;11(1):47–55.
42. Nam J, Carvalho MS. Flow in tensioned-web-over-slot die coating: effect of die lip design. *Chem Eng Sci*. 2010;65(13):3957–3971.
43. Koh H, Kwon I, Jung H, Hyun J. Operability window of slot coating using viscocapillary model for carreau-type coating liquids. *Korea-Aust Rheol J*. 2012;24(2):137–141.
44. Yang CK, Wong DSH, Liu TJ. The effects of polymer additives on the operating windows of slot coating. *Polym Eng Sci*. 2004;44:1970–1976.
45. Chu W-B, Yang J-W, Wang Y-C, Liu T-J, Tiu C, Guo J. The effect of inorganic particles on slot die coating of poly (vinyl alcohol) solutions. *J Colloid Interface Sci*. 2006;297:215–225.
46. Bhamidipati KL, Didari S, Harris TAL. Slot die coating of polybenzimiazole based membranes at the air engulfment limit. *J Power Sources* 2013;239(0):382–392.
47. Bhamidipati KL, Didari S, Bedell P, Harris TAL. Wetting phenomena during processing of high-viscosity shear-thinning fluid. *J Non-Newton Fluid*. 2011;166(12–13):723–733.
48. Hens J, Boiy L. Operation of the bead of a pre-metered coating device. *Chem Eng Sci*. 1986;41(7):1827–1831.
49. Chu W-B, Yang J-W, Liu T-J, Tiu C, Guo J. The effects of pH, molecular weight and degree of hydrolysis of poly (vinyl alcohol) on slot die coating of PVA suspensions of TiO_2 and SiO_2. *Colloid Surf A Physicochem Eng Asp*. 2007;302:1–10.
50. Yu W-J, Liu T-J. Reduction of the minimum wet thickness in extrusion slot coating. *Chem Eng Sci*. 1995;50:917–920.
51. Lin Y-T, Chu W-B, Liu T-J. Slot die coating of dilute suspensions. *Asia-Pac J Chem Eng*. 2009;4(2):125–132.
52. Ning C-Y, Tsai C-C, Liu T-J. The effect of polymer additives on extrusion slot coating. *Chem Eng Sci*. 1996;51:3289–3297.
53. Chin C-P, Wu H-S, Wang SS. Improved coating window for slot coating. *Ind Eng Chem Res*. 2010;49(8):3802–3809.
54. Lu S-Y, Lin Y-P, Liu T-J. Coating window for double layer extrusion slot coating of poly (vinyl-alcohol) solutions. *Polym Eng Sci*. 2001;41:1823–1829.
55. Lin Y-N, Liu T-J, Hwang S-J. Minimum wet thickness for double-layer slide-slot coating of poly(vinyl-alcohol) solutions. *Polym Eng Sci*. 2005;45:1590–1599.
56. Chu V, Tsai M-Z, Chang Y-R, Liu T-J, Tiu C. Effects of the molecular weight and concentration of poly(vinyl alcohol) on slot die coating. *J Appl Polym Sci*. 2010;116(2):654–662.
57. Han G, Lee S, Ahn W-G, Nam J, Jung H. Effect of shim configuration on flow dynamics and operability windows in stripe slot coating process. *J Coating Tech Res*. 2014;11(1):19–29.
58. Huang Y-C, Wang T-Z, Tsai C-P, Liu T-J. Operating window of solution casting, part I: Newtonian fluids. *J Appl Polym Sci*. 2013;129(1):507–516.
59. Snoeijer JH, Andreotti B. Moving contact lines: scales, regimes, and dynamical transitions. *Annu Rev Fluid Mech*. 2013;45:269–292.
60. Bonn D, Eggers J, Indekeu J, Meunier J, Rolley E. Wetting and spreading. *Rev Mod Phys*. 2009;81(2):739–805.
61. Blake TD, Ruschak KJ. A maximum speed of wetting. *Nature* 1979;282(5738):489–491.
62. Burley R, Kennedy BS. An experimental study of air entrainment at a solid/liquid/gas interface. *Chem Eng Sci*. 1976;31(10):901–911.
63. Gutoff EB, Kendrick CE. Dynamic contact angles. *AIChE J*. 1982;28:459–466.
64. Cohu O, Benkreira H. Air entrainment in angled dip coating. *Chem Eng Sci*. 1998;53(3):533–540.
65. Benkreira H, Khan MI. Air entrainment in dip coating under reduced air pressures. *Chem Eng Sci*. 2008;63:448–459.
66. Vandre E, Carvalho MS, Kumar S. Delaying the onset of dynamic wetting failure through meniscus confinement. *J Fluid Mech*. 2012;707:496–520.
67. Vandre E, Carvalho MS, Kumar S. On the mechanism of wetting failure during fluid displacement along a moving substrate. *Phys Fluids*. 2013;25(10).
68. Vandre E, Carvalho MS, Kumar S. Characteristics of air entrainment during dynamic wetting failure along a planar substrate. *J Fluid Mech*. 2014;747:119–140.
69. Chang HM, Lee CC, Liu TJ. The effect of bead vacuum on slot die coating. *Int Polym Proc*. 2009;24(2):157–165.
70. Pasquali M, Scriven LE. Free surface flows of polymer solutions with models based on the conformation tensor. *J Non-Newton Fluid*. 2002;108(1–3):363–409.
71. Lee AG, Shaqfeh ESG, Khomami B. A study of viscoelastic free surface flows by the finite element method: Hele-shaw and slot coating flows. *J Non-Newton Fluid*. 2002;108(1–3):327–362.
72. Huang Y-C, Wang T-Z, Liu T-J, Tiu C. Operating window of solution casting. II. Non-newtonian fluids. *J Appl Polym Sci*. 2015;132(5):41411.
73. Yamamura M. Assisted dynamic wetting in liquid coatings. *Colloids Surf A Physicochem Eng Asp*. 2007;311(1–3):55–60.
74. Yamamura M, Miura H, Kage H. Postponed air entrainment in dilute suspension coatings. *AIChE J*. 2005;51(8):2171–2177.
75. Nam J, Scriven LE, Carvalho MS. Tracking birth of vortex in flows. *J Comput Phys* 2009;228(12):4549–4567.
76. Nam J, Carvalho MS. Flow visualization and operating limits of tensioned-web-over slot die coating process. *Chem Eng Process*. 2011;50(5–6):471–477.
77. Lee S, Nam J. Analysis of slot coating flow under tilted die. *AIChE J*. 2015;61(5):1745–1758.
78. Romero OJ, Carvalho MS. Response of slot coating flows to periodic disturbances. *Chem Eng Sci*. 2008;63(8):2161–2173.
79. Tsuda T, de Santos JM, Scriven LE. Frequency response analysis of slot coating. *AIChE J*. 2010;56(9):2268–2279.
80. Perez E, Carvalho M. Optimization of slot-coating processes: minimizing the amplitude of film-thickness oscillation. *J Eng Math*. 2011;71(1):97–108.
81. Didari S, Ahmad ZY, Veldhorst JD, Harris TAL. Wetting behavior of the shear thinning power law fluids. *J Coating Tech Res*. 2014;11(1):95–102.
82. Feng JQ. Computational analysis of slot coating on a tensioned web. *AIChE J*. 1998;44(10):2137–2143.
83. Park E. *Physics of coating tensioned-web over slot die* [Ph.D. dissertation], University of Minnesota, 2008.
84. Weinstein SJ, Ruschak KJ. Coating flows. *Annu Rev Fluid Mech*. 2004;36:29–53.
85. Bhamidipati KL. *Detection and elimination of defects during manufacturing of high temperature polymer electrolyte membranes* [Ph.D. dissertation], Georgia Institute of Technology, 2011.

Manuscript received Sep. 26, 2015, and revision received Mar. 24, 2016.